DOI: 10.1016/S1872-5805(21)60034-3

Porous metal–organic frameworks for methane storage and capture: status and challenges

LI Dong-ze, CHEN Lei*, LIU Gang*, YUAN Zi-yun,
LI Bing-fan, ZHANG Xu, WEI Jia-qiang

(*Shandong Provincial key laboratory of Oil & Gas Storage and Transportation Safety, China University of Petroleum (East China), Qingdao* 266580, *China*)

Abstract: In the process of global transition to a sustainable low-carbon economy, the two major low-carbon energy technologies, namely, methane (CH_4) storage and methane capture face the same challenge, that is, the lack of efficient adsorbents. Metal-organic framework (MOF) materials have potential value in the field of gas adsorption storage because of their high specific surface area, good porosity, and adjustable pore structure. In this study, the structural design and synthesis methods of MOFs are introduced, and the research progress and problems associated with MOF materials in methane storage and capture are reviewed. The current research status of methane storage at high pressure is introduced in terms of volumetric and gravimetric uptake. For methane capture at atmospheric pressure, emphasis is placed on CH_4/N_2 and CO_2/CH_4 separation and methane capture technologies. Finally, the problems and challenges of using MOF materials to achieve efficient methane storage and capture are analyzed and future prospects are presented.

Key words: Metal-organic frameworks; Methane; Adsorption; Storage; Capture

1 Introduction

Natural gas, which is mainly composed of methane (CH_4), has been regarded as a substitute for traditional petroleum fuel for a long time because of its rich reserves and low carbon emissions, and the concept that it can replace gasoline and diesel as vehicle fuel has aroused widespread concern. In recent years, harmful contribution of methane as the second largest greenhouse gas has been paid progressively more attention to, and its ability to destroy the ozone layer is more than 20 times that of carbon dioxide (CO_2). According to the International Energy Agency (IEA), methane emissions from oil and gas industry reach 72 million tons in 2020[1]. In general, methane exists in the form of gas, and the volume energy density is only 0.036 MJ L^{-1}. Therefore, in order to take measures to increase the energy density or bulk density of methane, the focus is upon the capture and storage of methane. Adsorbed natural gas (ANG) technology based on porous adsorbents, has become a research hotspot in recent years. This method of natural gas storage requires low pressure and can be performed at room temperature. It has the advantages of good economy, convenient use, and high safety. The use of physical adsorption methods for methane recovery and emission reduction can also lead to significant reduction in the economic costs and improvement in the environmental benefits. The early selection of adsorbents was mostly concentrated on zeolite; nonetheless, it was difficult to achieve their high surface area beyond 1 000 m^2 g^{-1}, which resulted in limited adsorption of methane[2–3]. In contrast, activated carbon material has a relatively large surface area, and its methane uptake is obviously stronger than that of zeolite. In recent years, the study on activated carbon adsorption and storage of methane has also made tremendous progress. For example, the well-researched activated carbon AX-21 has a volumetric capacity of 203 cm^3(STP) cm^{-3} at 65 bar and a gravimetric capacity of 0.298 g g^{-1}[4], and the activated carbon LMA738 has a working capacity of 174 cm^3 (STP) cm^{-3}[5]. The gravimetric capacities of Maxsorb III and ACF (A-20) at 298 K and 1.4 bar are 25 and

Received date: 2021-02-06; **Revised date:** 2021-04-06

Corresponding author: CHEN Lei, Associate professor. E-mail: leo@upc.edu.cn;
LIU Gang, Professor. E-mail: liugang@upc.edu.cn

Author introduction: LI Dong-ze, Ph.D student. E-mail: B19060007@s.upc.edu.cn

18 mg g^{-1}, respectively[6]. However, porous carbon materials still have some significant limitations in the design of pore-size distribution, accessible surface area and pore volume, and surface functionalization[7], thus making it difficult to improve their methane storage capacity. As a result, a new generation of adsorbent materials is required to meet new index requirements.

Coordination polymer is a compound formed by self-assembly of metal ion and inorganic/organic ligand through coordination bond. At the beginning of the 18th century, the British Diesbach synthesized the earliest artificial coordination polymer, namely, ferric ferrocyanide ($Fe_4[Fe(CN)_6]_3$). As a type of coordination polymer, MOFs contain both organic ligands and potential pores, and have a higher specific surface area and porosity than traditional porous carbon materials (literature studies show that the highest Brunauer-Emmett-Teller (BET) specific surface area of MOFs materials is 8 318 m^2 g^{-1}[8], and the highest porosity reaches 94%[9]). Owing to the large selectivity of structural units (metal ions or clusters) and organic ligands of MOFs, the structures of MOFs are naturally varied and have pure organic or organic-inorganic hybrid pore surface, which leads to more abundant physical and chemical properties and great potential application prospects in the fields of adsorption and separation, catalysis, drug delivery, sensing, and so on. In the past 30 years, it has aroused extensive research interest of scholars.

MOFs have high specific surface area, high porosity, and open metal sites; thus, they offer great application potential in the fields of gas adsorption, such as methane storage, hydrogen storage, CO_2 capture, and so on. This study mainly reviews the latest research progress of MOFs in methane storage and capture in recent years.

2　Structural design and synthesis of MOFs

2.1　Characteristics of metal ions

The existence of unsaturated metal sites is one of the most important reasons for the strong adsorption of MOF materials. At present, most of the metal elements in the periodic table, except for the actinides, have been used to synthesize MOFs. Among them, univalent metal ions (Cu^+, Ag^+, etc.) belong to soft acids, which often need nitrogen-containing ligands to coordinate with them to form MOFs with sufficient stability. Moreover, in general, univalent metal ions are sensitive to external conditions (light, water, etc.) and are prone to redox process in the reaction systems. In contrast, bivalent metal ions (Cu^{2+}, Zn^{2+}, Mn^{2+}, Co^{2+}, Ni^{2+}, etc.) are the most commonly used metal ions for the synthesis of MOFs. These metals have moderated softness and hardness, and the coordination strength with ligands containing nitrogen and oxygen is not as strong as that of covalent bonds, but it is also relatively stable. The MOF materials formed by trivalent or tetravalent metal ions (Al^{3+}, Fe^{3+}, Cr^{3+}, Zr^{4+}, Hf^{4+}, etc.) are very stable for their strong polarization ability and close covalent bonds with oxygen-containing ligands; however, high valent metal ions react easily with water to form oxides and hydroxides, which, to a certain extent, hinders the growth of crystal, thus it is not easy to form large single crystals.

2.2　Characteristics of organic ligands

According to the definition of MOFs, ligands must be organic molecules with at least two or more coordination functional groups and multi-terminal coordination ability. The organic ligands of MOFs mainly include carboxyl, pyridine, azoles, and the mixed use of carboxylate and pyridine.

2.2.1　Carboxyl ligands

Carboxylate is a hard base, which can be coordinated with all types of common metal ions, in particular, trivalent and tetravalent metal ions to form bonds. With negative charge, carboxylate radical can neutralize the positive charge of metal ions and help to improve the stability of the MOFs. However, there exist many carboxylate coordination modes, which are difficult to predict and control. For example, the classical MOF material HKUST-1 was prepared by the reaction of Cu^{2+} with carboxyl ligand 1,3,5-benzenetricarboxylate (BTC (Fig. 1))[10]. HKUST-1 consisted of three-dimensional (3D) crossed square channels with a pore size of about 0.9 nm, which could keep the

framework stable after the removal of the water molecules of copper ligands by heating, for that reason, it had been widely studied and used in the fields of adsorption, storage, separation, and so on. Férey et al.[11] used BTC ligands and prepared MIL-101 framework, whose pore size (3.0–3.4 nm) was the largest of all the MOF materials at that time (Fig. 1). Based on this basis, Kim et al.[12] used the extended BTC ligand TATB to increase the maximum pore size of MIL-101 to 4.7 nm. The pore size of NOTT series synthesized by Schröder et al. using extended BTC ligands also exceeded 4.0 nm[13]. Consequently, the triangular BTC ligand and its extended structure have great advantages in constructing large-pore MOFs.

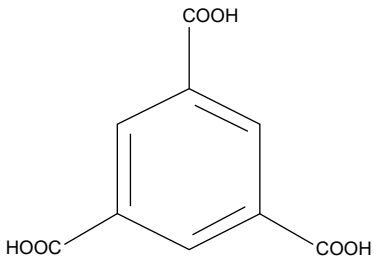

Fig. 1 Structure of BTC.

2.2.2 Pyridine ligands

Pyridines are also a type of ligand often used in the preparation of MOFs. The nitrogen atoms in pyridine ligands are under sp^2 hybridization state and contain a lone pair of electrons, thus the coordination mode is relatively simple and clear. However, the coordination ability of pyridine with most metal ions is weak, and pyridine ligands are not charged, which indicates that other components need to balance the positive charge of metal ions. Noteworthy, some polynuclear metal clusters contain both bidentate and monodentate end-capping ligands. Therefore, the pyridine functional group can be combined with carboxylate or a mixture of two ligands.

2.2.3 Azoles ligands

Azole ligands include imidazole, pyrazole, triazole, etc., which have the advantages of both carboxyl ligands and pyridine ligands. The coordination mode is simple and clear, in which the nitrogen atom is connected to the hydrogen atom, thus a proton can be removed to form an anionic multi-terminal ligand with strong alkalinity, which significantly improves the stability of the prepared MOFs[14]. Yaghi et al.[15–17] used Zn^{2+} or Co^{2+} to react with imidazole ligands to synthesize zeolite imidazolate framework (ZIF) series MOFs with a typical molecular sieve framework and becomes an important branch in the field of MOFs research (Fig. 2). Yaghi et al.[18] also used combinatorial chemistry to obtain topological types and structures that are not available in traditional molecular sieves. ZIF series materials have high specific surface area, high thermal stability, and excellent aqueous phase stability[20]. Moreover, the high pKa (acidity coefficient) value of N-H bond in azoles realizes the stable coordination bonds between metals and ligands under alkaline conditions, making azoles MOFs one of the few MOFs topologies that are not easy to decompose under strong alkali conditions. Pyrazole MOF (NiBDP-AgS) with Ag-S functional group (Fig. 3) constructed by Fei et al. could catalyze 10 cycles without deactivation under the action of up to 200 mol% of organic bases, such as DBU[19].

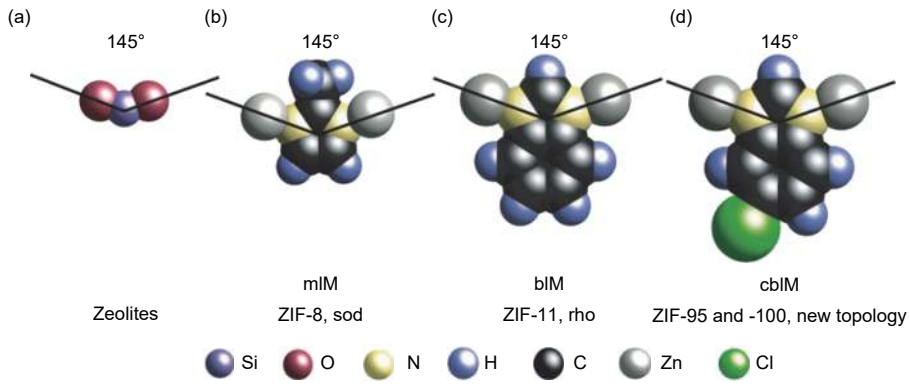

Fig. 2 Bridging angles and girths in zeolites and IMs[16]. Reproduced with permission.

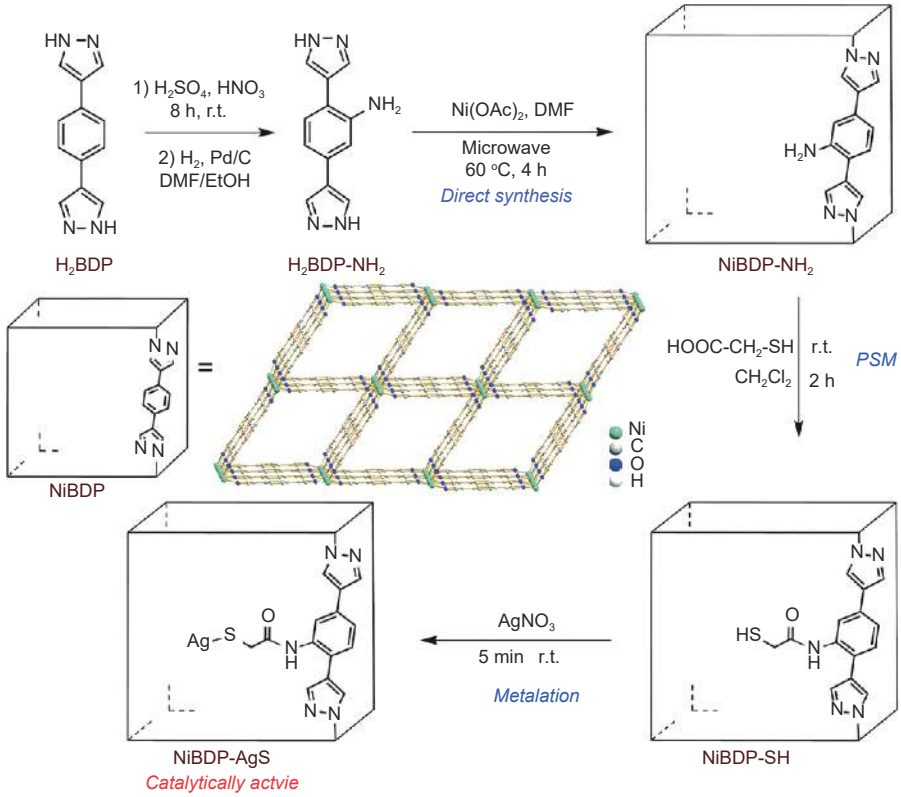

Fig. 3　Synthesis flow chart of NiBDP-AgS[19]. Reproduced with permission.

2.2.4　Mixed use of carboxylate and pyridine

Furthermore, the mixed use of carboxylate and pyridine can make up for the deficiency when used alone to meet the coordination and charge requirements of specific multinuclear metal clusters[21]. For example, M. J. Rosseinsky[22] used a mixture of BTC and 4,4'-bipyridine (bipy) to construct a stable and porous column-supported MOF (Fig. 4). In this MOF structure, carboxyl ligands are connected with each other to form a stable 2D structure, and nitrogen-containing pyridine ligands are connected to each 2D structure like a pillar to form a stable 3D structure. The porosity of the MOF reached 74%. Kitagawa[23] also used a similar method to synthesize MOF [Cu(tf-bdc)-(MeOH)] with better methane storage capacity.

2.3　MOFs synthesis method

2.3.1　Solvothermal method

Solvothermal method usually refers to the direct mixing of metal salts and organic bridging ligands in specific solvents (such as water or organic solvents), and then put into a closed high-pressure vessel (such as a reactor). Further, the reactants react when subjected to heat treatment under the autogenic pressure of the system, the reaction temperature is usually between 100 and 200 °C, and it usually takes half a day to several days for a reaction to complete[24]. The advantage of solvothermal method is that the higher temperature and pressure in the system are conducive to single crystal growth. By controlling the reaction conditions, MOFs single crystal suitable for X-ray diffraction experiments can be successfully obtained. However, the disadvantages including heating, high energy-consumption, and long reaction time are also obvious. Currently, most porous MOFs are synthesized under solvothermal conditions. Noteworthy, solvent often has guiding and template effects due to its complicated influence on the synthesis of MOFs.

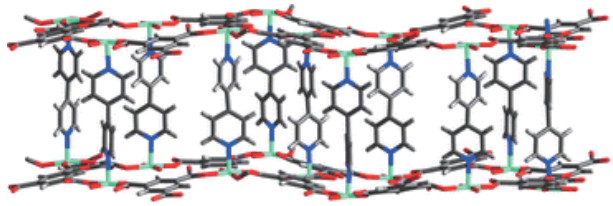

Fig. 4　The three-dimensional coordination polymer, showing the pillaring of adjacent (6,3) $Ni_3(btc)_2$ sheets by 4,4'-bipy ligands[22]. Reproduced with permission.

2.3.2 Ordinary solution method

Similar to the solvothermal method, the ordinary solution method refers to the mixing of metal salts and organic ligands in solvents (water or organic solvents), by stirring or allowing it to stand in an open system at a lower temperature (below 100 °C)[25]. The reactants gradually precipitate with the progress of the reaction. Although the common solution is energy-saving and easy to operate, the stability of the single crystal is poor, which is not conducive to crystal characterization, thus it is rarely used in the preparation of MOFs.

2.3.3 Solid-phase reaction method

The solid-phase reaction method refers to mixing and heating of metal oxides or hydroxides with organic ligands, and allowing it to react in the presence of a small amount of solvent or even without solvent to generate MOF with micron crystals. The reaction process does not rely excessively on the effect of the solvent; therefore, the solid-phase reaction method involves low cost and is beneficial to environmental protection. Tomislav[26] mixed ZnO with polyazole ligands, and synthesized a series of high-purity ZIF MOFs with uniform particle size by ball milling (Fig. 5).

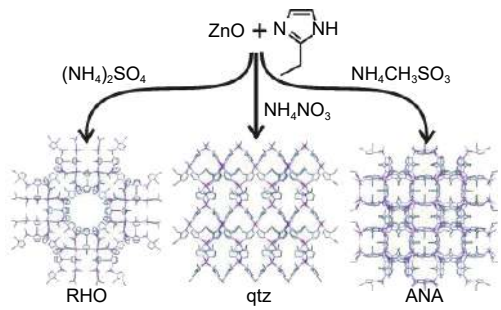

Fig. 5 ZIF series produced by solid-phase reaction method[26]. Reproduced with permission.

The yield of solid-phase reaction method was close to 100% and no other by-product except steam was produced. The prepared crystal was not only of excellent quality, but also exhibited better adsorption properties than the sample prepared by solvothermal method, and it was very easy to be mass produced. At present, international chemical enterprises have tried to carry out the commercial production[27–28].

2.3.4 Diffusion method

Diffusion method refers to the dissolution of the reactants in the same or different solvents. Through certain control, the two fluids containing the reactants are in contact with each other through diffusion at the interface or in a specific medium, thereby reacting and forming products. The diffusion method usually has a low reaction rate, a long reaction time, and is difficult to carry out the synthesis on a large scale, thus this method is rarely used for the preparation of MOFs.

For the research and application of MOF materials, the ideal synthesis method should have at least the following characteristics:

(1)The size of the single crystal produced should be suitable;

(2)Simple operation, less time-consuming, high repeatability, and large-scale production;

(3)Environmentally friendly and cost effective.

2.3.5 Microwave method

In order to overcome the shortcomings such as inefficiency, time-consuming, and energy-consuming of traditional solvothermal method, microwave method is increasingly used[29–30]. For instance, Wang et al.[31] reviewed in detail the following characteristics of microwave method: (1) Shorter reaction times; (2) Smaller particle sizes; and (3) Selective synthesis of MOF. A number of studies has shown that, compared to solvothermal method, microwave method leads to the formation of MOF with better adsorption performance and selectivity[32–37].

2.3.6 Electrochemical method

The electrochemical method is a mild and rapid synthesis method, which provides the metal ions required for the reaction through anode dissolution. It has the advantages of short synthesis time, mild conditions, simple operation, and no requirement for metal salts[38]. Mueller et al.[39] arranged bulk copper plates with thickness of 5 mm, as anodes in an electrochemical cell with the carboxylate linker; 1,3,5-benzenetricarboxylic acid dissolved in methanol as solvent; and a copper cathode, to synthesize HKUST-1 using an electrochemical route. Noteworthy, this method can be used to prepare not only powder materials, but also MOF membrane materials[40–41].

2.3.7 Sonochemistry method

Sonochemistry is a fast developing branch of chemistry, which takes advantage of the ultrasound (US) power[42]. Sonochemistry method is based on the effect of the acoustic cavitation, which results in extreme local heating, high pressures, and very short lifetimes[43–44]. In order to achieve shorter reaction times, phase-selectivity and smaller particle sizes, sonochemical synthesis of MOFs is becoming progressively more popular. Starting from the synthesis of $(Zn_3BTC_2)\cdot 12H_2O$ by Qiu et al. in 2008[45], more and more researches on successful fabrication of MOFs by applying a sonochemical method have been reported[46–47].

2.3.8 Post-synthesis modification

MOFs have shown excellent designability to a considerable extent; notably, the addition of special groups and certain specific functions can be realized by controlling the raw materials required for synthesis. However, owing to the complexity of the synthesis reaction, it is impossible to achieve the addition of all the required functional groups by controlling the raw materials. Therefore, the method of post-synthesis modification has emerged as an effective strategy. The so-called post-synthesis modification involves the modification of the framework through some chemical reaction on the premise of maintaining the original framework, so that the framework has better functional groups and active centers, in order to achieve excellent functional properties[48]. The simplest post-synthesis modification can be understood as removing the easy-to-leave end-capping ligands on the synthesized MOF metal sites by heating, subjecting to vacuum, and by other methods to form coordinated unsaturated metal sites. Noteworthy, the post-synthesis modification of MOF should refer to the chemical modification of the metal center and organic bridging ligand after removing the easy-to-leave end-capping ligand.

Krista et al.[49] reported the synthesis of two types of MOFs, $[Cu_3(MBTC)_2(H_2O)_3]_n$ (MBTC denotes methyl-1,3,5-benzenetricarboxylate) and $[Cu_3(EBTC)_2(H2O)_3]_n$ (EBTC denotes ethyl-1,3,5-benzenetricarboxylate), using HKUST-1 modified with methyl ($-CH_3$) and ethyl ($-C_2H_5$) groups, and the adsorption isotherms of CO_2, methane, and water vapor were measured at 298 K. It was found that the uptake of two types of MOFs was similar to that of HKUST-1 at low pressure (lower than 5 bar); however, the water absorption was obviously lower than that of HKUST-1 due to the existence of functional groups $-CH_3$ and $-C_2H_5$.

2.4 Structure screening and design of MOFs

MOFs are extremely designable due to their composition of multiple combinations of metal nodes, organic linkers, and functional groups, thus it is not feasible to perform experimental characterization on tens of thousands of MOFs. With the rapid improvement of computing power of advanced computer systems, the use of molecular simulation methods to design and screen MOF materials with specific applications can significantly save manpower and material resources[50]. Many scholars have used molecular simulation methods for multiple application areas of MOFs, such as methane storage[51–54], hydrogen storage[55–57], CO_2 capture[58–59], and other related applications[60–65]. Most of the researches used the Grand Canonical Monte Carlo (GCMC) method to study the adsorption behavior of MOFs toward guest molecules. Compared to experimental characterization, although molecular simulation has greatly simplified the screening and design process of the MOF structure, it also takes days or even weeks to calculate the adsorption characteristics of one MOF material. Thus, it is not realistic to carry out simulation for all MOFs in a huge database.

In recent years, machine learning methods have also emerged as an effective way to pre-screen materials and accelerate large-scale simulation of workflow. Structural characteristics such as pore volume and specific surface area are the most commonly used parameters to describe the structure-performance relationship of MOFs[51, 53, 66]. Supervised learning, as a method of machine learning, can use these geometric properties to predict gas uptake in MOFs and highlight the most important features in future design[60, 67, 69]. For instance, Woo et al.[68] reported the first quantitative structure-property prediction model with structur-

al parameters as descriptors based on big data's analysis method, and predicted the methane uptake of 130 000 hypothetical MOFs at 298 K and 1, 35, and 100 bar, respectively. Srivastava et al.[70] introduced chemical descriptors, in addition to structural descriptors, for adsorption analysis. George et al.[71] introduced average Boltzmann factors to characterize the adsorption capacity of materials based on the structural parameters, which resulted in significant improvement of the prediction accuracy, in particular, under low pressure. Machine learning and big data mining technology can make full use of a large amount of data generated by high-throughput screening, which can not only accelerate material simulation, but also provide a deeper understanding of the trend of structural performance. Structural parameters cannot reflect the most essential characteristics of material adsorption capacity; therefore, the bottleneck to improve the accuracy of big data's method in screening MOFs structure is to search for more suitable descriptors.

3 Methane adsorption mechanism of MOFs

The storage mechanism of MOFs is mainly based on physical adsorption; however, for methane adsorption, mainly two types of strong adsorption sites exist[72]: open and unsaturated metal ion (cluster) coordination sites and potential pocket sites. Open metal site is one of the main features that distinguish MOFs from other porous adsorbent materials. Methane molecules coordinate with open metal sites through electrostatic interaction, which makes the metal sites become one of the main adsorption sites. Noteworthy, the adsorption capacity of a single metal site depends not only on its affinity toward adsorbate molecules, but also on its geometry. After studying the optimized geometry of NTA-Ca and NTA-Mg (Fig. 6), Martin et al.[73] found that the surface of the adsorbent formed by the coordination of unsaturated Mg^{2+} with terminal oxygen atom was triangular plane, while the surface of adsorbent formed using unsaturated Ca^{2+} coordinated with terminal oxygen atom was triangular vertebrae, and the surface of triangular cone prevented the NTA ligand to completely encapsulate larger Ca^{2+}, so that it could be partially exposed. Each Ca^{2+} could adsorb three to four methane molecules. Mg^{2+} could only adsorb one.

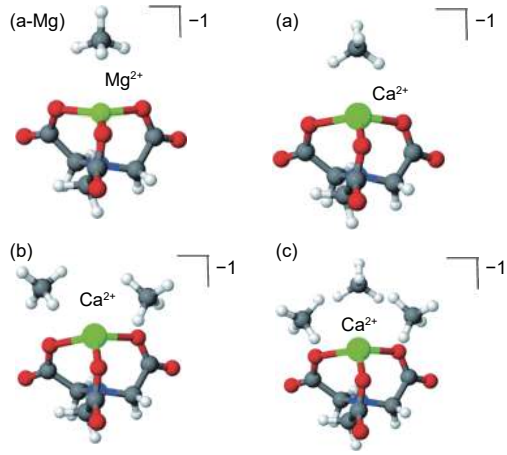

Fig. 6 Clusters formed by NTA-Mg (a-Mg), NTA-Ca (Amurc) and CH_4. The first adsorbed CH_4 blocked the adsorption site of NTA-Mg, while the conical NTA-Ca could adsorb three CH_4[73]. Reproduced with permission.

Metal sites as strong adsorption sites of MOF are widely recognized and easily accepted. In many cases, however, expected methane uptake measured by experiments is not possible even if all open metal sites are combined with guest molecules. Thus, theoretically, there should be other strong adsorption sites in MOF, besides metal sites. Zhou et al.[72] comprehensively explored the mechanism of methane adsorption by using three landmark MOFs, namely, HKUST-1, PCN-11, and PCN-14 (Fig. 7). They found that, in addition to the open metal sites that had long been recognized, the pockets at the hole-cage junction were also one of the strong adsorption sites for guest molecules, where the guest molecules could come into contact with multiple surfaces and the van der Waals interaction was enhanced (Fig. 7). Interestingly, this van der Waals force enhancement phenomenon existed only in the small cages and their pockets, while the large cages with relatively flat pore surfaces hardly bound methane. This indicated that enriching the open metal sites, increasing the proportion of accessible cages and channels, and minimizing the proportion of macropores were beneficial to increase the total methane adsorption of MOFs.

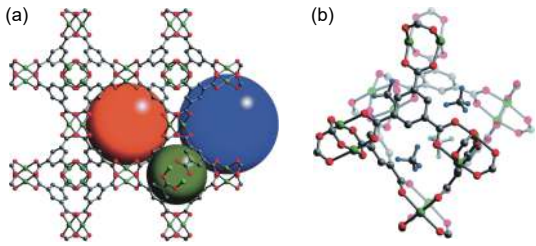

Fig. 7　(a) Three types of cages in HKUST-1, and their diameters are 0.5 nm (dark green), 1.1 nm (orange) and 1.35 nm (blue); (b) The green, gray, red and light blue spheres of CD4 molecules adsorbed at the four holes of the octahedral cage represent Cu, C, O and D atoms, respectively[4]. Reproduced with permission.

4　Methane storage under high pressure

Methane is abundant in nature, has the largest H/C ratio among all hydrocarbons, and produces the least CO_2 after combustion, thus it is considered to be a type of high-quality clean energy which can replace crude oil, coal, and other traditional energy sources. Under conventional conditions, the volume energy density of methane is only 0.036 MJ L^{-1}, which is only about 1/1 000 of that of traditional fuels such as gasoline and diesel. At present, the main storage methods of natural gas as automotive fuel include high pressure storage (room temperature, pressure above 200 atmospheric pressure) and liquefaction storage (atmospheric pressure, 112 K). Although these two methods can significantly improve the volume energy density of methane and the related technologies have been relatively mature, the high-pressure and low-temperature storage mode consumes a large amount of energy and is low in safety. In order to store methane efficiently and safely, many traditional porous materials, including zeolite and activated porous carbon, have been studied and evaluated. However, the methane storage capacity of these materials is not ideal because of their limited pore volume and specific surface area. Owing to its large specific surface area and large pore volume, MOF material is considered as a promising candidate material for methane storage[74–75]. Moreover, using MOFs material for methane storage has the advantages of good economy and high security, thus it is a research hotspot in recent years.

In 1997, Kitagawa et al.[76] prepared 3D framework with channeling cavities-$\{[M_2(4,4'\text{-bpy})_3(NO_3)_4 \cdot H_2O]\}_n$ (M = Co, Ni, Zn), and carried out the first methane adsorption experiment based on this material at 298 K and pressure in the range of 1–36 bar. In 1999, Yaghi[77–78] prepared MOF-5 ($Zn_4O(BDC)_3$), which could keep the framework stable after removing solvent molecules, and IRMOF series was further synthesized by introducing organic groups based on the MOF-5. It was proved that this series had good methane uptake tendency at room temperature and 36 bar. The research carried out by the two pioneers, namely, Kitagawa and Yaghi, clarified the huge application value and potential of MOF materials in the field of methane storage, laying the foundation for subsequent research and pointing out the direction.

In order to enable ANG storage technology to be practically applied to vehicles, the United States Department of Energy (DOE) has set a goal for the adsorption and storage of methane at room temperature. The volumetric storage density should not be less than 0.155 g cm^{-3} (equivalent to 263 cm^3 cm^{-3}) and the gravimetric storage density should not be less than 0.5 g g^{-1} (equivalent to 700 cm^3 g^{-1}).

In order to meet the DOE standards, many MOFs, including IRMOF series[77–80, 87], NOTT series[81], UTSA series[82], aluminum-based MOFs[83–84], HKUST-1[10], Ni-MOF-74[85], PCN-14[86], etc., have all been used to study methane adsorption and storage performance[68]. In the past ten years, MOFs material storage methane technology has made several breakthroughs one after another. Some scholars prepared MOFs that could meet the requirements of volumetric storage density or gravimetric storage density, respectively. However, MOF materials that can meet the two indicators at the same time at room temperature and appropriate pressure have not been prepared yet.

4.1　Fundamental concept of methane storage

4.1.1　Excess, absolute and total adsorption

In the research of methane adsorption based on MOF materials, the following three concepts define the amount of adsorption: excess adsorption, absolute adsorption, and total adsorption (Fig. 8). Excess adsorption refers to the amount of guest molecules adsorbed on the surface of the material pores; absolute

adsorption refers to the amount of guest molecules without gas-solid interaction in the adsorption area; and total adsorption refers to the amount of all guest molecules in the pores, including excess adsorption and the guest molecules without gas–solid interaction. The relationship among excess uptake, absolute uptake, and total uptake can be described by using the following three formulas[50]:

$$n^{t} = n^{e} + v^{0}\rho$$
$$n^{a} = n^{e} + v^{a}\rho$$
$$v^{a} = v^{0} - v$$

Where n^{t} is total uptake, n^{a} is absolute uptake, n^{e} is excess uptake, v^{0} is void volume, v is gas volume, v^{a} is adsorbed phase volume, and ρ is gas density. The excess uptake is measured experimentally, and the others can be calculated from the above-mentioned equations.

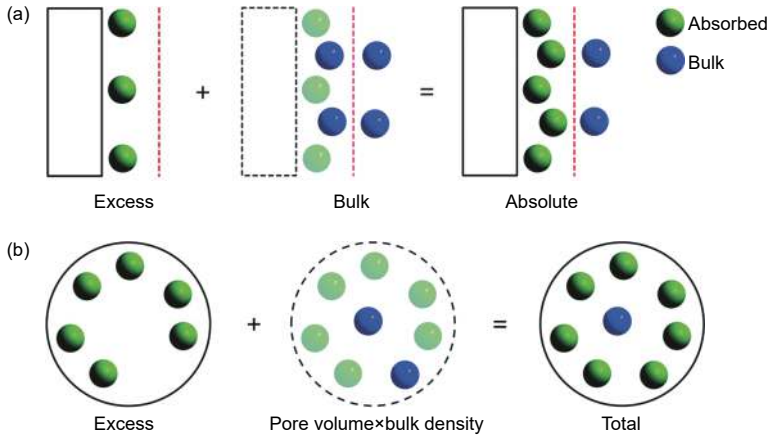

Fig. 8 Schematic diagram of excess adsorption, absolute adsorption and total adsorption (the left side of the red line is the adsorption area, the right side of the red line is the unadsorbed area, the green sphere represents the adsorbed molecules, and the blue sphere represents the unadsorbed molecules)[4]. Reproduced with permission.

4.1.2 Volumetric and gravimetric uptake

Volumetric uptake and gravimetric uptake are the two important indicators to measure the adsorption performance of adsorbent materials. The volumetric uptake refers to the volume of methane adsorbed per unit volume of adsorbent at standard temperature and pressure, and the gravimetric uptake refers to the mass of methane adsorbed per unit mass of adsorbent. For automotive applications, owing to the limited space of the fuel tank, the volumetric uptake of the adsorbent is more demanding; however, the excessive weight of the adsorption device leads to the increase in the energy consumption. Therefore, how to find a balance between the volumetric and gravimetric uptake is next challenge to be overcome urgently for methane storage.

4.1.3 Deliverable capacity

In addition to the above-mentioned concepts, deliverable capacity is also a key indicator to measure the methane storage capacity of MOFs and their practical application value, which refers to the available uptake calculated based on the difference between the high-pressure uptake and the low-pressure uptake. It is necessary for automobile to drive enough methane fuel from the fuel tank to the engine under the lowest pressure limit (usually 5 bar). Considering economy benefits, the highest pressure that a single-stage or two-stage compressor can provide is usually 35 or 65 bar[15], thus the difference in uptake between 5–35 bar/65 bar is usually defined as the deliverable capacity of methane storage materials[50]. In some researches, the upper limit pressure is set to 80 and 100 bar, respectively[83–84].

4.2 Influencing factors of methane adsorption

4.2.1 Adsorption conditions

Adsorption conditions (mainly pressure and temperature) are important factors to determine the total uptake. Adsorption storage of methane belongs to physical adsorption, which is an exothermic process. Thus decreasing temperature is conductive to the adsorption process; however, increasing pressure can promote the collision probability of gas molecules on

the adsorption surface, which is also an effective way to improve the adsorption capacity. Noteworthy, in practical industrial applications, deliverable capacity is more important than the total uptake, and the decrease of temperature brings the increase of the total uptake, but it is likely to be counterproductive to the deliverable capacity. Chen et al.[7] summarized the methane storage capacity of many types of MOFs at 270 and 298 K (Fig. 9), and found that for the MOFs with small pore volume (0.5−0.9 $cm^3\ g^{-1}$), the deliverable capacity at 270 K was lower than that at 298 K, and when the pore volume increased gradually, the decrease of temperature showed a positive effect on the deliverable capacity. This was attributed to the fact that the smaller pore volume led to higher bare metal site density, and compared to that at high pressure, the decrease of temperature resulted in more obvious increase of the uptake below 5 bar. This resulted in the decrease of deliverable capacity. Importantly, increasing pressure could improve the deliverable capacity of MOF materials, but only in a limited way. For example, the deliverable capacity of NiMOF-74 was 142, 152, 160 cm^3 (STP) cm^{-3} at 65, 80, and 100 bar[4, 7]. Higher storage pressure makes the vehicle storage tank heavier and larger, which brings additional cost, space, and safety problems, thus limiting its practical application.

4.2.2　Material structure

It is generally accepted that the gravimetric uptake of methane is basically proportional to the pore volume and/or BET surface area of MOF (Fig. 10 (a)) at room temperature [80, 88]. However, the larger the pore volume and the smaller the density of MOF, the less conducive it is to the increase of volumetric uptake. Therefore, theoretically, an upper limit of volumetric uptake exists, as shown in Fig. 10 (b). Moreover, Chen et al.[7] also proposed an empirical formula for calculating volumetric uptake at 298 and 270 K and 65 bar.

$$C_{\text{total}} \times D_{\text{c}} = (-100.557 \times V_{\text{p}}^2 + 439.799 \times V_{\text{p}} - 2.640) / (1.022 \times V_{\text{p}} + 0.360) \quad (298\text{K})$$

$$C_{\text{total}} \times D_{\text{c}} = (-70.463 \times V_{\text{p}}^2 + 460.543 \times V_{\text{p}} - 2.709) / (1.022 \times V_{\text{p}} + 0.360) \quad (270\text{K})$$

Where C_{total} is the total methane adsorption at room temperature and 65 bar, cm^3 (STP) cm^{-3}; and D_{c} and V_{p} are the density and pore volume of MOFs.

4.2.3　Mechanical properties

Noteworthy, at present, the volume uptake of al-

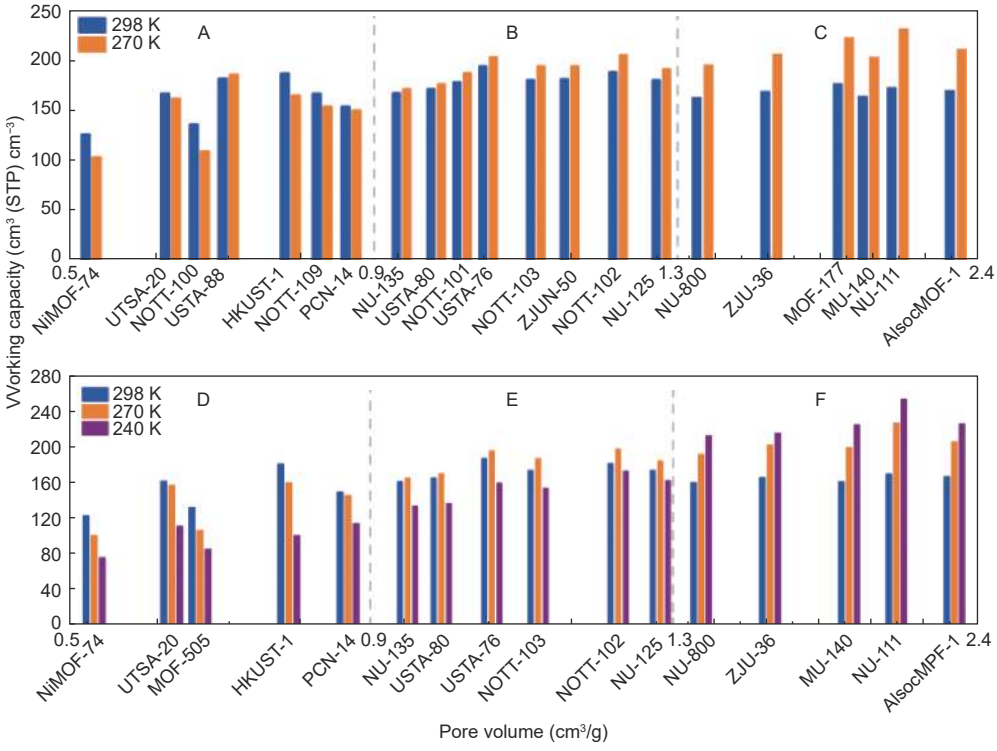

Fig. 9　Comparison of deliverable capacity at different storage temperatures (5−65 bar)[7]. Reproduced with permission.

most all MOF to methane is calculated based on the perfect single crystal density, which is theoretically the maximum. In practical application, the large number of gaps between the powder filling the fuel tank leads to the significant reduction in the density, resulting in a lower volume uptake. For example, the single crystal density of MOF-5 is 0.621 g cm^{-3}, while the density of stacked powder is 0.13 g cm^{-3}[89]. Therefore, the adsorbent particles should be compacted in practical application, taking this into account. Comprehensive understanding of the basic relationship between frame structure and mechanical properties is expected to be of great value for the design and synthesis of MOF materials, which can be compacted to a high enough density without affecting the methane uptake[90]. More importantly, better control over the size and shape of MOF particles is required. In particular, Researches on compacted activated carbon show that higher packing density can be achieved when two or more particles of different sizes are mixed and pressed at the same time[4].

4.3 Volumetric uptake

HKUST-1, a typical example of MOF materials, has attracted the maximum research attention in this field. Its framework consists of a 3D network structure with tbo topology formed by the connection of $Cu_2(-COO)_4$ unit and tricarboxylic acid ligand (BTC^{3-}), as shown in Fig. 11[10, 93]. The BET specific surface area of HKUST-1 is 1 850 m^2 g^{-1} and the volume is 0.78 cm^3 g^{-1} through the N_2 adsorption experiment at 77 K. Hupp et al.[91] found that the volumetric uptake of HKUST-1 at 298 K and 6.5 MPa reached 267 cm^3 cm^{-3} through the methane adsorption experiment, and exceeded the volumetric adsorption target set by DOE. HKUST-1 is one of the known MOF materials with the highest volumetric uptake.

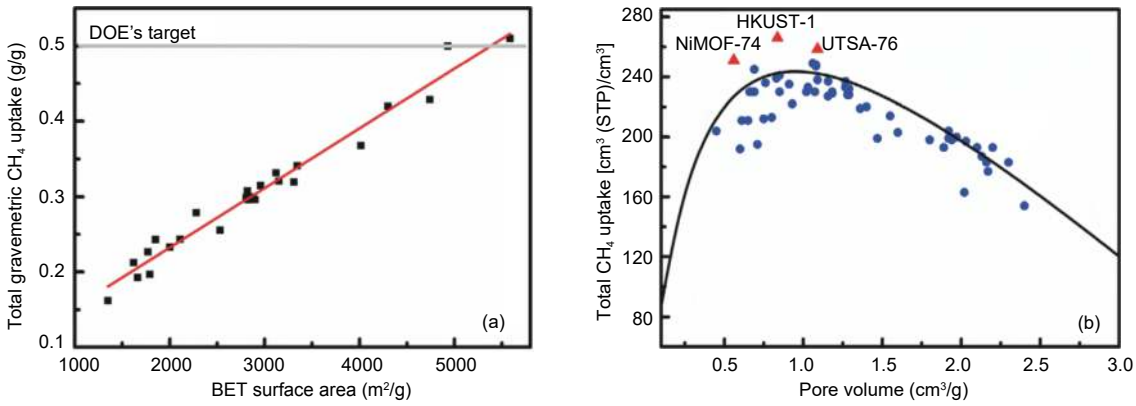

Fig. 10 (a) Relationship between gravimetric uptake and BET specific surface area at 270 K; (b) Relationship between volumetric uptake and pore volume at 298 K[7]. Reproduced with permission.

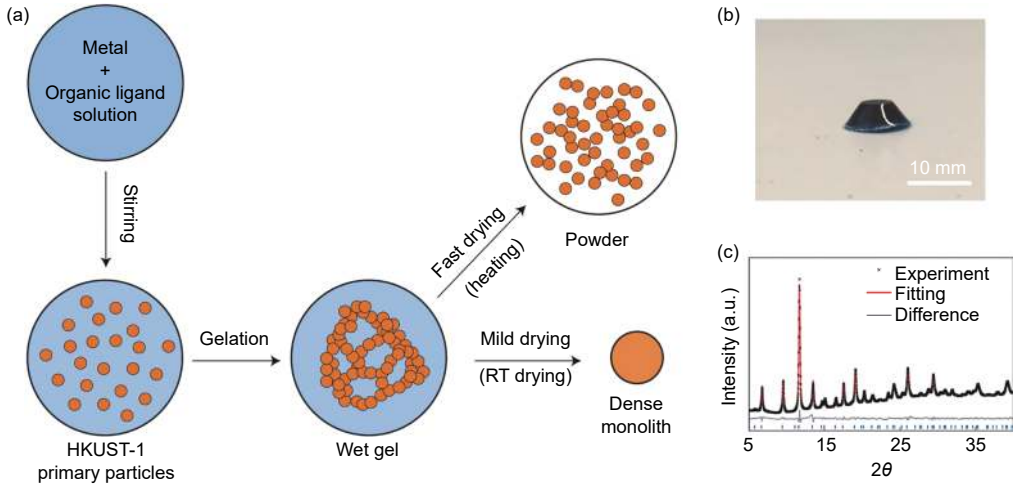

Fig. 11 Schematic representation of monolithic and powder MOF synthesis[92]. Reproduced with permission.

However, it is a pity that the gravimetric uptake of HKUST-1 is only 0.216 g, which is much lower than the target of DOE, thus limiting its application in vehicle methane storage. Moreover, as mentioned above, the volumetric uptake of HKUST-1 is actually calculated based on the perfect single crystal density, and the density decrease caused by the stacking effect is not taken into account. Furthermore, after experimental densification, the internal pore structure mechanically partially collapses, and the uptake gets reduced by 35%.

David et al.[92] prepared $_{mono}$HKUST-1 by the sol-gel method (Fig. 11). After experimental densification, it was found the volumetric uptake reached 259 cm^3 cm^{-3}, which was very close to the target of DOE. $_{mono}$HKUST-1 showed good mechanical properties, and the hardness was 130% higher than its conventional MOF counterparts. However, the gravimetric uptake was only 0.177 g g^{-1} at 298 K and 6.9 MPa.

Chen et al.[81] tested the methane adsorption performance of a series of MOF materials (NOTT-100a, NOTT-101a, NOTT-102a, NOTT-103a, and NOTT-109a) at 300 K and 35 bar. The result showed that NOTT-101a, NOTT-102a, and NOTT-103a exhibited excellent deliverable capacities of methane (136−140 cm^3(STP) cm^{-3}, 5−35 bar), and they derived an empirical equation to predict the methane storage performance of previously reported microporous MOF materials of V_p less than 1.50 cm^3 g^{-1}.

$$C = -126.69 \times V_P^2 + 381.62 \times V_P - 12.57$$

where C is the excessive gravimetric methane storage capacity at 35 bar and 300 K, cm^3 (STP) g^{-1} and V_p is the pore volume of a MOF material, cm^3 g^{-1}. This empirical formula provides a convenient method to screen MOFs for methane storage purpose.

Compared to other porous adsorbent materials, one of the advantages of MOF is that certain specific functions can be realized by introducing functional groups. It was found that introduction of certain groups on ligands could significantly improve the uptake of MOF materials. For example, Zhou et al.[86] prepared a nbo topology structure MOF, PCN-14 ([$Cu_2(H_2O)_2$(adip)][H_4adip=5,5'-(9,10-anthryl)di-isophthalic acid]), constructed using $Cu_2(-COO)_4$ unit and anthracene ring-containing tetracarboxylic acid ligand $adip^{4-}$, N_2 adsorption experiment at 77 K exhibited that the BET specific surface area of PCN-14 was 2 000 m^2 g^{-1}, and the pore volume was 0.85 cm^3 g^{-1}[91]. The methane uptake at 298 K and 6.5 MPa reached 230 cm^3 cm^{-3}, which is a considerable value, and has been the highest record for the volumetric uptake of MOF materials adsorbing methane for a long time. The reason for the enhanced uptake is believed to be the introduction of large aromatic rings on the ligand, the pore channel structure consisting of nano-sized pore cages, and the presence of unsaturated metal ion active sites on the pore channel surface.

Chen et al.[7, 82] prepared NOTT-101 and UTSA-76 [$Cu_2L(H_2O)_2$·5DMF·H_2O] with pyrimidine nitrogen atom on the ligand, as shown in Fig. 12. At 298 K and 6.5 MPa, the volumetric uptake of NOTT-101 was 237 cm^3 cm^{-3}, while that of UTSA-76 was 257 cm^3 cm^{-3}. The difference between the two is only the presence of nitrogen atoms on the ligand of UTSA-76; therefore, Chen et al. believed that introducing Lewis basic pyridine and pyrimidine nitrogen atoms into the ligand could improve the methane adsorption and storage capacity of the MOF materials, and UTSA-76 with a functional nitrogen site provides additional functional sites as secondary adsorption sites, which can enhance the interaction with methane molecules, thereby increasing total uptake and deliverable capacities.

Chen et al.[94] introduced a multifunctional pyrimidine ring to the UTSA-76 linker, designed and synthesized a new ligand (H4L), and expanded the synthesis of nbo type MOF, namely, UTSA-110. After testing, it was found that the gravimetric uptake of UTSA-110 at 298 K and 65 bar was 0.288 g g^{-1}, and the volumetric uptake was 241 cm^3(STP) cm^{-3}. Although the volumetric uptake of UTSA-110 was lower than that of UTSA-76 under the same conditions, the deliverable capacity (5.8–65 bar) was higher than those of UTSA-76 and HKUST-1 (UTSA-110: 190 cm^3 (STP) cm^{-3}, UTSA-76: 187 cm^3(STP) cm^{-3}, and HKUST-1: 183 cm^3(STP) cm^{-3}).

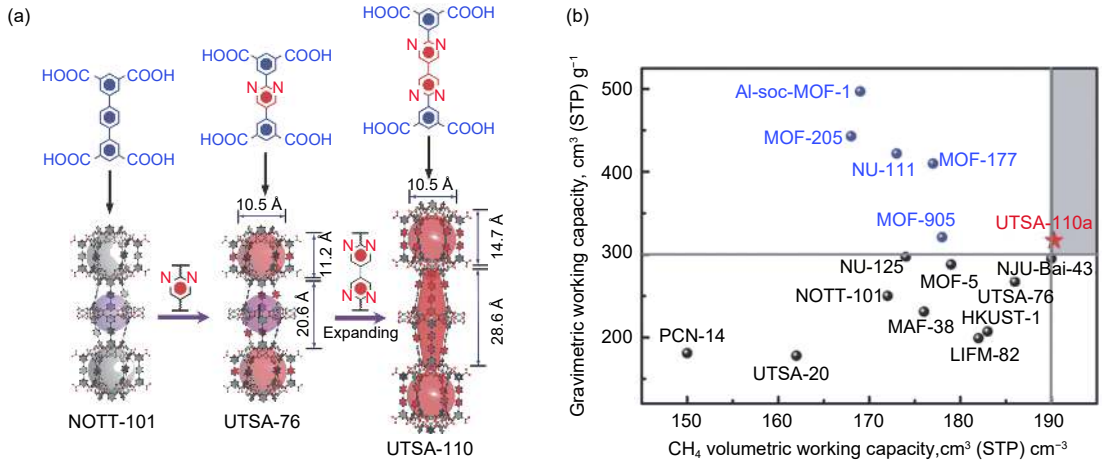

Fig. 12 (a) Crystal structure of NOTT-101, UTSA-76 and UTSA-110; (b) Comparison of USTA-110 methane gravimetric/volumetric uptake with other MOFs at 298 K and 65 bar[94]. Reproduced with permission.

In recent years, significantly more research attention has been paid to the deliverable capacity of adsorbents, which is more important for practical applications. Yaghi et al.[95] analyzed a series of MOFs (including MOF-905, MOF-905-Me_2, MOF-905-Naph, MOF-905-NO_2, and MOF-950) produced by the reaction of secondary building units $Zn_4O(–CO_2)_6$ and benzene-1,3,5-tri-β-acrylate and tested them for methane adsorption. The test results showed that this series of materials exhibited a good deliverable capacity, among them, the capacity for MOF-905 reached 203 cm^3 (STP) cm^{-3} at 298 K and 80 bar. Yaghi et al. believed that due to the moderate isosteric enthalpy of adsorption (Qst) of MOF-905, the methane adsorption under 5 bar was only 25 cm^3(STP) cm^{-3}, which was much lower than that of 72 cm^3(STP) cm^{-3} under HKUST-1.

Mason et al.[96] found that Co(bdp) could adjust its structure according to the change of external pressure due to its elasticity, which resulted in significant improvement in the methane uptake at low pressure, and optimized the methane adsorption process (Fig. 13). Its volumetric uptake was 203 cm^3(STP) cm^{-3}, and its deliverable capacity reached 197 cm^3(STP) cm^{-3}, at 298 K and 65 bar. The adsorption isotherm also showed "s" shape different from that of other rigid MOFs (Fig. 13). This flexible framework provided a new research idea for improving the deliverable capacity of MOF materials.

In previous studies, it was generally believed that open metal sites (OMSs) played a very important role during the process of adsorption of methane by MOFs. For example, Zhang et al.[97] prepared MAF-38 with OMSs that exhibited high methane uptake, and the volumetric uptake reached 263 cm^3(STP) cm^{-3} at 298 K and 65 bar (Fig. 14). The simulation results showed that the appropriate pore size/shape and strong organic binding sites enhanced the interaction between host–guest and guest–guest molecules, thus providing extremely high adsorption enthalpy and effective utilization of pore space. These results have a certain guiding significance for the development of new gas storage adsorbent materials.

Although the above-mentioned MOF materials such as HKUST-1, UTSA-76, and PCN-14 have excellent methane volumetric uptake or deliverable capacity, the gravimetric uptake is less than 0.3 g g^{-1}, which is far from the target of DOE. The excessive material density limits its application as vehicle-mounted energy storage material.

4.4 Gravimetric uptake

MOF materials with large apertures tend to have high gravimetric storage density; however, the poor interaction between guest molecules and the frame surface limits the volumetric storage density. On the other hand, due to the strong interaction between guest molecules and the surface of small aperture MOF materials, the volumetric storage density is often considerable; nonetheless, the relatively low pore volume limits the gravimetric storage density[97].

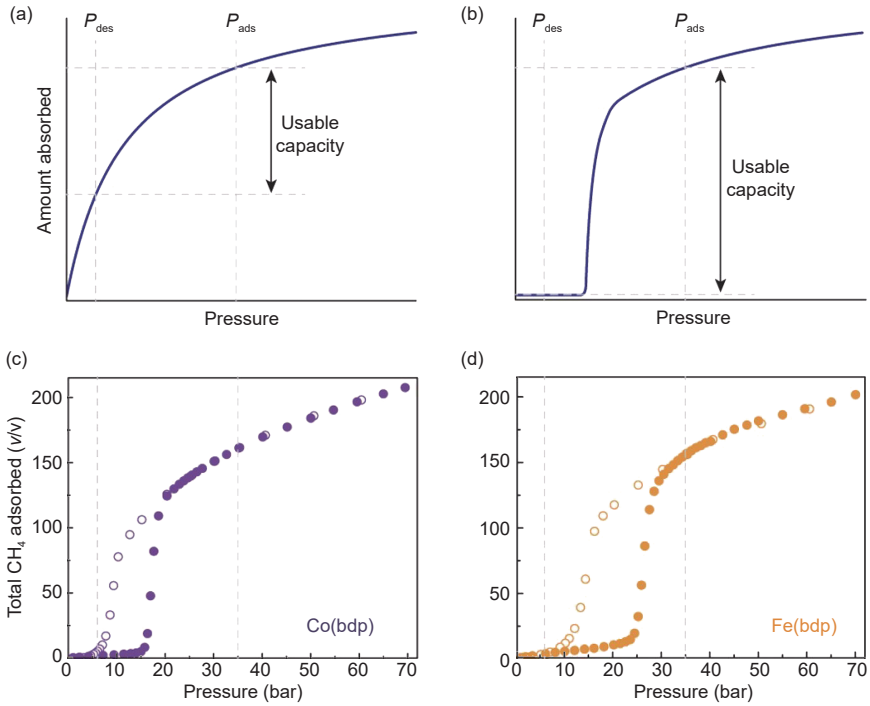

Fig. 13　Comparison of deliverable capacity between (a) rigid MOFs and (b) flexible MOFs; Total CH_4 uptake of (c) Co (bdp) and (d) Fe (bdp) at 25 ℃[96]. Reproduced with permission.

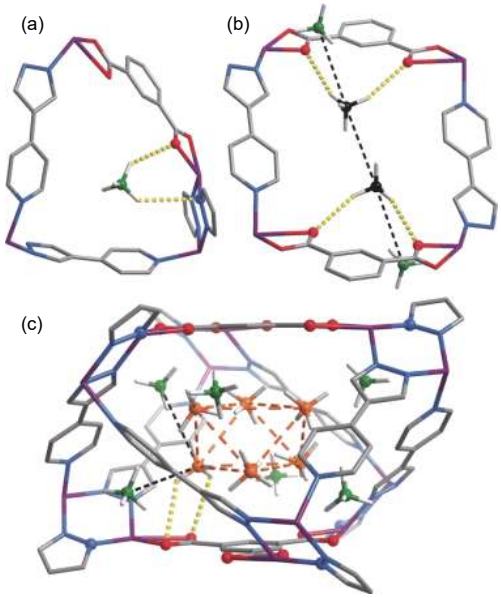

Fig. 14　The (a) primary (green), (b) secondary (black), and (c) ternary (orange) CH_4 adsorption sites in MAF-38[97]. Reproduced with permission.

Therefore, the way to balance the gravimetric and volumetric uptake of MOF materials as vehicle energy storage materials is an urgent challenge for researchers.

In 2016, Chen et al.[7] systematically evaluated and compared the reported methane storage capacity of MOFs at 298 and 270 K, and found that by slightly lowering the storage temperature to 270 K could significantly increase the methane volumetric and gravimetric uptake (Fig. 15). The results of adsorption test of NU-111 and MOF-177 at 270 K and 65 bar indicated that the gravimetric uptake could reach 0.5 and 0.43 g g^{-1}, and the deliverable capacity could also reach 239 and 230 cm^3(STP) cm^{-3}. Among them, the adsorption data of NU-111 were consistent with research results provided by K. Omar, and showed high reliability[98]. However, Chen et al. only met the gravimetric uptake target at 270 K, which was still far from the room temperature required by DOE.

Alezi et al.[83] applied the molecular building block method to construct a series of novel xoc topology aluminum-based MOFs (Al-soc-MOF-1, Al-soc-MOF-2, Al-soc-MOF-3), with high porosity and stability. Among them, Al-soc-MOF-1 exhibited an excellent methane gravimetric uptake: 0.42 g g^{-1} at 298 K and 65 bar, reaching 84% of the DOE target.

Omar et al. devoted extensive research efforts on balancing the gravimetric and volumetric uptake of methane and achieved breakthrough results. They tested the methane adsorption characteristics of six most promising MOF materials, including PCN-14, UTSA-20, HKUST-1, Ni-MOF-74 (Ni-CPO-27), NU-

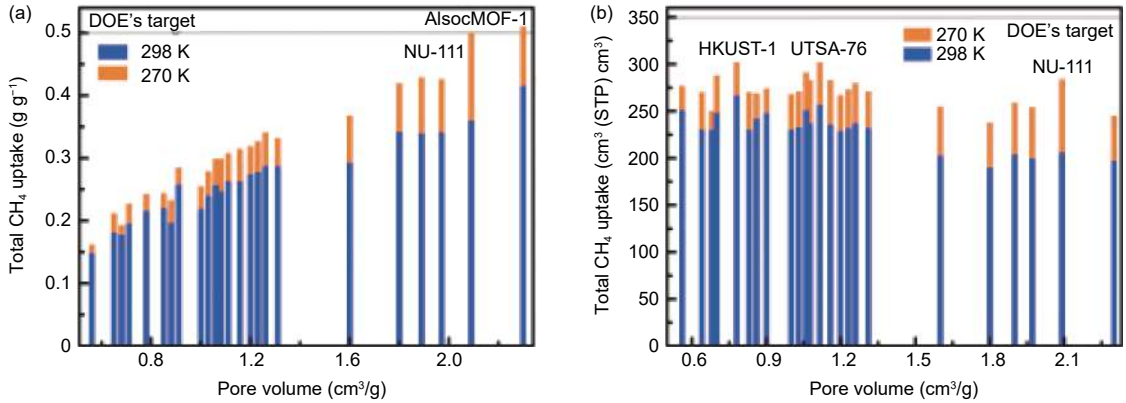

Fig. 15 Comparison of gravimetric/volumetric absorption of MOFs at 270 K and 298 K[7]. Reproduced with permission.

111, and NU-125, and also found the excellent volumetric uptake of KHUST-1, revealing that NU-111 could achieve 75% of both gravimetric and volumetric targets. According to the law of linear correlation among the gravimetric uptake, pore volume, inverse density, and specific surface area of MOF materials, Omar et al. estimated that a MOF with surface area of 7 500 $m^2\ g^{-1}$ and pore volume of 3.2 $cm^3\ g^{-1}$ could reach the current DOE gravimetric target of 0.5 g g^{-1}, while simultaneously exhibiting around ~ 200 $cm^3\ cm^{-3}$ volumetric uptake achieved at 6.5 MPa[91]. Based on this result, they added a benzene ring to the original organic ligand of NU-1500, and prepared two MOF materials, namely, NU-1501-Al and NU-1501-Fe by solvothermal method[99]. The results showed that the methane gravimetric uptake of NU-1501-Al at 296 and 270 K was as high as 0.54 g g^{-1} and 0.66 g g^{-1}, the volumetric uptake was 214 cm^3(STP) cm^{-3} and 262 cm^3 (STP) cm^{-3}, respectively, and the deliverable methane uptake at 0.5–10 MPa was 198 cm^3(STP) cm^{-3} and 238 cm^3(STP) cm^{-3}, which thus successfully achieved the DOE targets. However, as mentioned above, increasing pressure is not the best choice to improve the gas storage capacity of adsorbents, and the high pressure of 10 MPa is also a great burden on vehicle compressors. Table 1 lists the structural parameters and methane uptake of some MOFs under high pressure.

4.5 Issues and prospects

At this stage, the bottleneck of MOF materials as adsorbents for vehicle ANG technology is that it is difficult to meet both volumetric uptake and gravimetric uptake at the same time. Moreover, traditional experiments and molecular simulation methods are inefficient and poorly targeted. In recent years, extensive use of big data analysis methods has provided a fast and accurate way for the pre-screening of MOF materials. The big data method is expected to efficiently screen out MOF materials that meet the targets from database based on the most essential characteristics of MOFs gas storage performance. However, meeting the volumetric and gravimetric uptake is only the goal of the first stage, in order to realize the large-scale industrial application of vehicle ANG technology, the following problems need to be solved:

4.6 Increase in deliverable capacity

Compared to the total uptake, the deliverable capacity is more important in practical applications. Through structural design, the introduction of functional groups and other operations can significantly increase the total uptake of the adsorbent; however, it may also more significantly increase the adsorption of methane at lower pressures, which instead reduces the deliverable capacity. In recent years, flexible MOFs with "breathing effect" have been proposed, whose structure can be optimized and adjusted according to external pressure, thus significantly reducing the amount of methane adsorption at low pressure, and is expected to solve this problem.

4.7 Heat management due to the exothermic/endothermic nature of the adsorption–desorption phenomena

The temperature change during the adsorption–desorption process definitely has a negative impact on the deliverable capacity of the MOF materials and

Table 1　Examples of MOF materials for methane storage.

Materials	BET($m^2\ g^{-1}$)	V_p($cm^3\ g^{-1}$)	CH_4 total uptake				CH_4 excess uptake(mg g^{-1})				Delivery($cm^3\ cm^{-3}$)
			mg g^{-1}	$cm^3\ cm^{-3}$	T(K)	P(bar)	mg g^{-1}	$cm^3\ cm^{-3}$	T(K)	P(bar)	
Al-soc-MOF-1[83]	5590	2.30	410	197	298	65	-	-	-	-	201(5–80 bar)
Co(bdp)[96]	2911(Langmuir)	-	-	203	298	65	-	-	-	-	197
HKUST-1[100-101]	1850	0.78	216	267	298	65	178	220	298	65	190
$_{mono}$HKUST-1[92]	1193	0.52	177	267	298	69	151	227	298	69	172
LIFM-82[102]	1624	0.71	210	271	298	80	-	-	-	-	217(5–80 bar)
MAF-38[97]	2022	-	247	263	298	65	-	-	-	-	187
MFM-115a[103]	3394	1.38	278	238	298	65	-	-	-	-	191
MIL-53(Al)[104]	1100	0.59	⩾96	155	304	35	-	-	-	-	
MIL-53(Cr)[104]	1100	0.56	⩾96	165	304	35	-	-	-	-	-
MIL-10[p0(Cr)[105]	1900	1.10	152	150	303	60	-	-	-	-	-
MIL-101(Cr)[105-106]	4230	2.15	217.6	135	303	60	-	-	-	-	-
MOF-5[107]	3800	1.55	-	132	298	35	~ 160[108]	-	300	60	-
MOF-177[95]	4700	1.83	-	208	298	80	-	-	-	-	185(5–80 bar)
MOF-200[80]	4530	3.59	-	-	-	-	234	-	298	80	-
MOF-210[80]	6240	3.6	-	-	-	-	264	-	298	80	157(5–80 bar)
MOF-519[84]	2400	0.928	190	259	298	65	-	-	-	-	230(5–80 bar)
MOF-905[95]	3490	1.34	270	206	298	65	-	-	-	-	203(5–80 bar)
MOF-905-Naph[95]	3640	1.39	-	211	298	80	-	-	-	-	184(5–80 bar)
MOF-905-Me_2[95]	3310	1.25	-	217	298	80	-	-	-	-	188(5–80 bar)
MOF-905-NO_2[95]	3380	1.29	-	203	298	80	-	-	-	-	177(5–80 bar)
MOF-950[95]	3440	1.30	-	209	398	80	-	-	-	-	174(5–80 bar)
Ni-MOF-74[91, 100]	1350	0.51	148	251	298	65	125	210	298	65	129
NJU-Bai43[109]	3090	1.22	283	254	298	65	-	-	-	-	198
NOTT-101a[81, 94]	2805	1.08	247	237	298	65	-	-	-	-	181
NU-111[91, 98]	4930	2.09	360	205	298	65	262	150	298	65	179
NU-125[91]	3120	1.29	287	232	298	65	223	181	298	65	183
NU-135[110]	2600	1.02	219	230	298	65	-	-	-	-	170
NU-1500-Al[99]	3560	1.46	290	200	296	65	-	-	-	-	181(5–80 bar)
NU-1501-Al[99]	7310	2.91	410	163	296	65	-	-	-	-	174(5–80 bar)
NU-1501-Fe[99]	7140	2.90	400	168	296	65	-	-	-	-	176(5–80 bar)
PCN-14[91, 112]	2000	0.85	197	230	298	65	157	183	298	65	157
PCN-66[114]	4000	1.63	-	187	398	65	177.6	110	298	35	152
PCN-68 [115]	5109	2.13	-	187	298	65	185.6	99	298	35	157
UTSA-20[91]	1620	0.66	181	230	298	65	150	191	298	65	170
UTSA-76[82, 113]	2820	1.09	263	257	298	65	-	-	-	-	197
UTSA-110a[94]	3241	1.263	288	241	298	65	-	-	-	-	190
ZIF-8[108]	-	-	~ 85	-	300	36	70	-	300	36	-
ZJU-70 [114]	1791	0.676	-	211	298	65	-	-	-	-	-

ANG system. The heat transfer performance of MOFs and the integration method of ANG system thermal management technology with the existing vehicle thermal management system will also be the focus of the next step.

Moreover, the efficient packing of the adsorbent materials in the storage tank, impurity tolerance (such as C_2H_6, C_3H_8, CO_2, H_2O, etc.), recyclability (100 cycles), adsorbent cost (<\$10 kg^{-1}), etc. are also the challenges to be overcome urgently in the industrial application of ANG technology.

5　Methane capture under atmospheric pressure

Methane, as a clean energy source, produces only CO_2 and water after combustion, which reduces pollutant emissions from the source. However, methane is a short-lived strong greenhouse gas with a rapid warming effect, and its greenhouse effect is more than 20 times that of CO_2[115]. Methane emissions are the

second largest cause of global warming today. A report issued by the Intergovernmental Panel on Climate Change pointed out that deep reduction of non-CO_2 greenhouse gases such as methane was a necessary condition for controlling global warming below 1.5–2 °C[116]. Methane emissions come from a variety of man-made and natural resources, in the energy sector, including oil, natural gas, coal, and bio-energy. The latest comprehensive estimate released by the IEA in September 2019 indicated that the global annual methane emissions were about 570 Mt (million tons), which included emissions from natural sources (about 40% of emissions). Emissions from human activities accounted for the remaining 60%, and the oil and gas sector emitted 82 Mt[1]. Alvarez et al.[117] estimated that the U.S. O/NG supply chain emitted 13 Tg y^{-1} of methane. Methane is often less concerned than CO_2. Despite the initial industry-led measures and the government's policies and regulations, methane emissions still stay at a high level. Fig. 16 and 17 show the predicted and actual methane emissions from the oil and gas industry in recent years. Therefore, achievement of rapid and large-scale reduction of methane emissions is still a huge challenge.

In the past, it has been reported that biofiltration is used to purify methane produced by landfills[120–125]. However, biofiltration is more complex in optimizing the process parameters of long-term operation[123], and it is more suitable for small landfills[124-126]. Methane has resource attributes; therefore, good control of methane is to make good use of it, which can significantly improve resource utilization and bring huge economic benefits. The IEA pointed out that 75% of methane reduction in the oil and gas industry was technically feasible, and 45% of methane reduction could achieve net zero cost[1, 128]. Almost all links of the oil and gas supply chain are responsible for methane emissions[117], and different mitigation strategies for emissions can be selected according to the types of emitters. For storage tanks and well casinghead vent emissions, methane can be recovered using vapor recovery unit, whose adsorbent traditionally consists of porous carbon materials[127]. Some studies reported the related results of CO_2 and methane capture with porous carbon materials[6, 129–137]. For example, Mofarahi et al.[138] reported that the methane uptake of zeolite 5A reached 7.456 mg g^{-1} at 303 K and 0.99 bar. Kim et al.[6] studied the methane adsorption characteristics of two different activated carbon types, namely, Max-

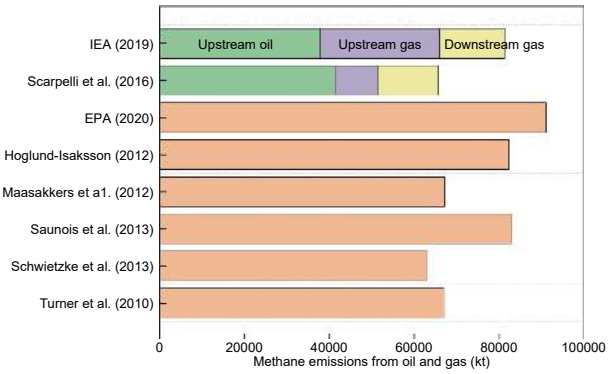

Fig. 16 Methane emissions from oil and gas, comparison of IEA and other estimates[118].

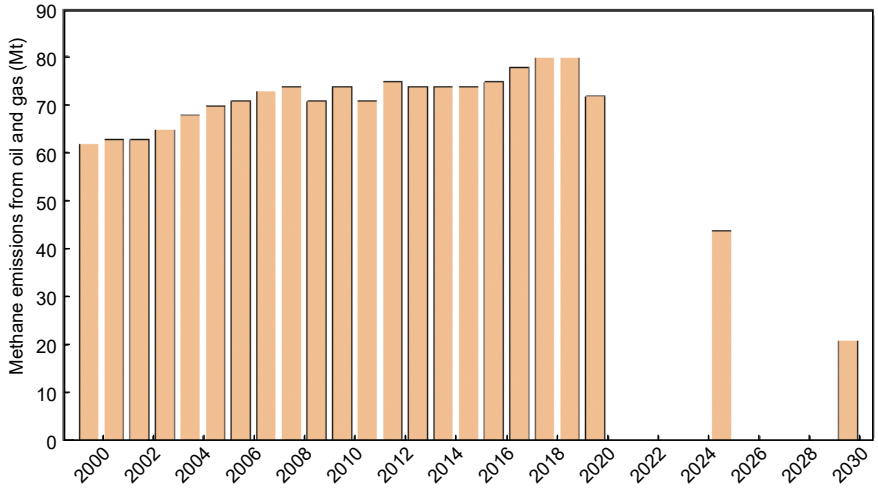

Fig. 17 Oil and gas sector methane emissions 2000-2030 in the Sustainable Development Scenario[119].

sorb III and ACF (A-20). The adsorption capacities of the two activated carbon materials were 25 and 18 mg g^{-1} at 298 K and 1.4 bar, respectively. Noteworthy, the adsorption capacity is closely related to the specific surface area and porosity of porous materials. For methane capture, the volumetric uptake is more important than the gravimetric uptake, and more attention has been paid to volumetric uptake. Theoretically, the total uptake is closely related to the specific surface area and porosity of porous materials. Owing to structural limitations, it is difficult to achieve the specific surface area of zeolites beyond 1 000 m^2 g^{-1}, and the ionic properties of zeolites are not conducive to methane adsorption. Porous carbon materials represented by activated carbon for methane storage and capture are limited by pore size, specific surface area, and surface functionalization[7, 139].

The large specific surface area, high porosity, and structural design characteristics of MOF materials endow them with unique advantages in the field of gas adsorption storage, in particular, in reducing leakage emissions caused by station equipment malfunction and storage tank breathing loss emissions. Previous research focused on methane storage under high pressure; however, to achieve reduction in methane emission, the research should focus on the adsorption characteristics of methane under room temperature and atmospheric pressure.

5.1 CH_4/N_2 separation

In order to make full use of valuable resources and slow down the trend of global warming, recovering methane from different impurity sources can provide a lot of environmental and economic benefits, which has recently aroused widespread interest in the research community. Nitrogen and methane have very similar physical and chemical properties. The separation of CH_4/N_2 is widely regarded as one of the most challenging technical problems in the utilization of various natural gas resources. Importantly, cryogenic distillation is a commonly used technology for industrial CH_4/N_2 separation; however, it requires higher energy consumption and operating costs, and is not flexible in many small-scale applications[140]. To overcome this challenge, a series of adsorption-based separation strategies has been developed. However, most traditional adsorbents, such as zeolites and porous carbon materials, encounter problems such as low selectivity or unsatisfactory capacity[141–144]. Thus, MOF materials have been widely studied as an adsorbent for gas separation.

5.1.1 Fundmental concept of CH_4/N_2 separation

(1) Adsorption selectivity

The actual pressure swing adsorption or temperature swing adsorption process requires not only a high uptake of the adsorbent, but also certain separation selectivity in order to meet certain separation requirements. A simple method to determine the adsorption selectivity of materials based on adsorption isotherms is Henry's law constant method. This method involves the calculation by using the slope ratio of the lower uptake of two gases in the low pressure region. The Ideal Adsorbed Solution Theory proposed by Myers and Prausnitz in 1965 can be used to more accurately calculate the separation selectivity coefficient of the mixture from the gas adsorption isotherm of a single component[145].

(2) Sorbent selection parameter

The sorbent selection parameter (SSP) is a comprehensive separation performance index that is used to evaluate and reflect the cyclic properties of the adsorption process, which was first proposed by Rege and Yang[146]. After being popularized by Bae et al.[147], it has been widely used in evaluation of cyclic pressure-swing adsorption (PSA) and vacuum-swing adsorption (VSA) process. SSP can be calculated by using the following formula:

$$S_{sp} = \frac{(S_{A/B}^{ads})^2}{S_{A/B}^{des}} \times \frac{\Delta N_A}{\Delta N_B}$$

where $S_{A/B}^{ads}$ and $S_{A/B}^{des}$ refer to the selectivity under adsorption–desorption conditions; ΔN_A and ΔN_B refer to the working capacity of two adsorbates, respectively.

5.1.2 Progress of separation of CH_4/N_2 based on MOFs

Li et al.[148] studied the adsorption behavior of methane and N_2 in 22 different MOFs by Monte Carlo

molecular simulation method. The results showed that the adsorption isotherm obtained by simulation was in good agreement with the experimental data. For the adsorption of methane and N_2, the adsorption amount was mainly determined by using the adsorption point and the smaller pore space. Compared to N_2, methane was preferentially adsorbed on all MOFs, which was consistent with the law of isotherm adsorption thermal reaction, in particular, under low pressure. Under low gas adsorption load, the adsorption of methane was mainly controlled by the interaction between adsorbate and framework caused by small pores.

Seda et al.[149] used molecular simulations to evaluate the CH_4/N_2 separation performance of 102 different MOFs, and provided the ideal parameters of MOFs as a CH_4/N_2 separation adsorbent: the maximum cavity diameter was in the range of 0.46–0.54 nm, the pore limiting diameters were in the range of 0.24–0.37 nm, the specific surface area was less than 2 000 $m^2\ g^{-1}$, and the porosity was less than 0.5.

Wang et al.[150] were inspired by the strong reducibility of formic acid and used the strong oxidation of metal nitrate to initiate the redox reaction process, and thus synthesized the metal-formate frameworks (MFFs) material, namely, Ni-FA ($[Ni_3(HCOO)_6]$). This method does not require solvents and template reagents, and can achieve simple, rapid, and low-cost synthesis of MOF materials, which is denoted as solvent-free explosive synthesis. Wang et al. used GCMC simulation technology and experimental research to study the adsorption performance of Ni-FA. The results showed that Ni-FA exhibited excellent selectivity and adsorption capacity for capturing methane from the CH_4/N_2 mixed system, and the methane uptake at 298 K, 1bar was 12.8 mg g^{-1} (33.97 $cm^3\ cm^{-3}$).

Wang et al.[151] synthesized two MOFs, namely, Co-MA-BPY and Ni-MA-BPY with good framework flexibility and a narrow and uniform pore network. Further studies showed that Co(Ni)-MA-BPY molecular sieve showed good stability toward water and humid air. Pure gas adsorption experiments showed that both of them were endowed with excellent methane absorption capacity (The values for Co and Ni-MA-BPY are 0.92 and 1.01 mmol g^{-1}, respectively) at 298 K and 1 bar, and higher CH_4/N_2 separation performance (values for Co and Ni-MA-BPY were 7.2 and 7.4, respectively), which was a very promising adsorbent. Table 2 summarizes the methane uptake and CH_4/N_2 separation performance of some MOFs for methane at room temperature and atmospheric pressure.

Table 2 Examples of CH_4 adsorption and separation from CH_4/N_2 (100 kPa).

Materials	CH_4 total uptake (mmol g^{-1})	CH_4/N_2 selectivities	Temperature (K)
Al-CDC[161]	1.44	13.1	298
ATC-Cu[159]	2.90	9.7	298
CAU-8-BPDC[152]	0.85	4.9	298
CAU-21-BPDC[152]	0.99	11.9	298
$[Co_3(C_4O_4)_2(OH)_2]$[153]	0.41	12.5	298
Co-MA-BPY[151]	0.92	7.2	298
Co-MOF-74[154]	1.91	3.2	298
Cu-MOF[160]	0.64	10.8	298
Mg-MOF-74[154]	1.66	1.5	298
MIL-100(Cr)[154]	0.60	3.0	298
MOF-5[155]	0.13	1.13	298
MOF-177[155]	0.56	4.0	298
Ni-MA-BPY[151]	1.01	7.4	298
$[Ni_3(HCOO)_6]$[156]	0.82	6.2	298
PCN-222[157]	0.35	4.8	298
$V_2Cl_{2.8}$(btdd)[158]	1.00	27*	298

*represents N_2/CH_4 selectivity

In addition to the data presented in Table 2, Liu et al.[161] also sorted out the CH_4/N_2 separation performance data of some MOF materials, which were quoted as a supplement, as shown in Fig. 18.

5.2 CH_4/CO_2 separation

Impurities such as H_2O, H_2S, and CO_2 need to be removed from natural gas before pipeline transportation. Similarly, biogas, which is a multicomponent gas mixture produced at atmospheric pressure principally composed of methane and CO_2, requires purification (>95% purity methane with only trace amounts of H_2S) before it can be transported by pipelines or stored in gas tanks[162–163]. MOFs constitute a relatively new class of materials, which exhibits great potential in the application of CO_2/CH_4 separation. Table 3 presents the CO_2 uptake and CO_2/CH_4 separation performance of some typical MOFs.

The variety of metal nodes, organic linkers, and network topologies makes the number of MOF al-

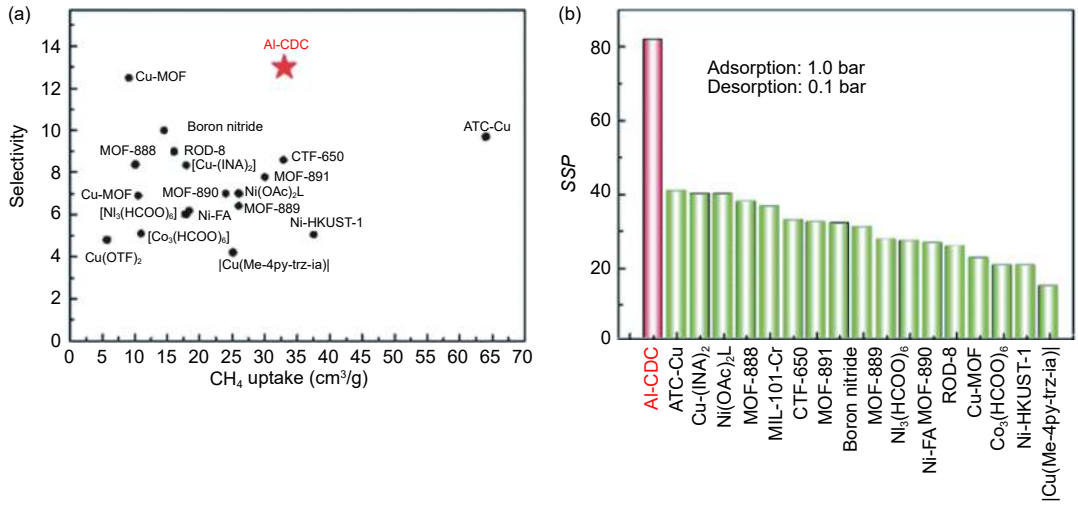

Fig. 18　(a,b) Comparison of CH_4/N_2 separation performance of some MOFs summarized by Liu[161]. Reproduced with permission.

Table 3　Typical examples of CO_2/CH_4 separation.

Materials	CO_2 total uptake (mol kg^{-1})	CO_2/CH_4 selectivities	Pressure (kPa)	Temperature (K)
IITKGP-6[164]	1.67	5.1	100	295
Cu-MOF[165]	-	6	100	303
MIL-53(Al)[166]	4.3(3.5bar)	4.10	100–3500	303
UTSA-16[167]	4.2	29.8	200	296
Mg-MOF-74[168]	8.56	105.1	200	296
CuBTC[169]	5.27	7.4	200	296
MIL-101[169]	2.16	9.6	200	296
SIFSIX-2-Cu[170]	1.85	5.3	100	298
SIFSIX-2-Cu-i[170]	5.41	33	100	298
SIFSIX-3-Zn[170]	2.55	231	100	298

most limitless. Thus, computational screening is an effective method to quickly search for target MOFs[171].

Seda et al.[172] combined GCMC method and molecular dynamics simulations to screen 3 794 MOF membranes for CO_2/CH_4 separation. The most promising MOF membranes offered the best combination of CO_2 permeability (>10^6 Barrer) and CO_2/CH_4 selectivity (>80), which outperformed polymeric membranes for CO_2/CH_4 separation. The results showed that MOFs had great potential in CO_2/CH_4 separation.

Wilmer et al.[66] carried out GCMC simulations to screen more than 130 000 hypothetical MOFs to investigate CO_2/CH_4 (50%/50%) separation efficiency at T = 298 K and various pressures. They found that MOFs with small pores and high CO_2 heat of adsorption were suitable for VSA separation, while MOFs with macropores were suitable for PSA separation.

However, previous studies investigating biogas purification often assumed that biogas is a binary 50%/50% mixture of methane and CO_2. Zhong et al.[173] performed molecular simulations to investigate the effect of trace amount of water on CO_2 capture in natural gas upgrading process in a diverse collection of 25 typical MOFs. The results showed that the effect of water on the adsorption selectivity of CO_2/CH_4 depended on the interaction between water molecules and MOFs. i.e., the stronger the interaction between the water molecules and the MOFs was, the greater the effect was. For a more realistic separation application, Siepmann et al.[174] carried out GCMC simulation of five-component (CH_4(50%)/CO_2(45%)/N_2(3%)/H_2S(1%)/NH_3(1%)) mixtures at T = 298 K and p = 0.1 bar and 1 bar. JOSNAG_clean was identified as a promising candidate to be considered for upgrading biogas. Firlej et al.[175] carried out high-throughput GCMC screening of nearly 3 000 existing MOF materials for CO_2/CH_4 separation in the presence of water at ambient conditions (p = 1 bar, T = 298 K), and variable gas humidity (0, 5%, 30%, and 40%), and the final selection revealed 13 most promising MOFs structures. One noteworthy factor is that MOFs that possess high CO_2/CH_4 selectivity usually have a very narrow PLD (< 0.4 nm).

5.3　Methane capture

Compared to the studies on the separation and capture of methane from CH_4/N_2 and CH_4/CO_2 mixed components, relatively few studies on the capture of single methane component have been reported. Ma et al.[159] reported a methane nano-trap based on ATC-Cu

that featured oppositely adjacent open metal sites and dense alkyl groups (Fig. 19). It could induce strong interaction with methane and provide excellent methane adsorption and separation performance. The methane nano-trap based on ATC-Cu exhibited record-high methane uptake (46.4 mg g^{-1}) and CH_4/N_2 selectivity at 298 K and 1 bar, thereby providing a new perspective for capturing methane to recover fuel and reduce greenhouse gas emissions.

In order to capture low-concentration methane

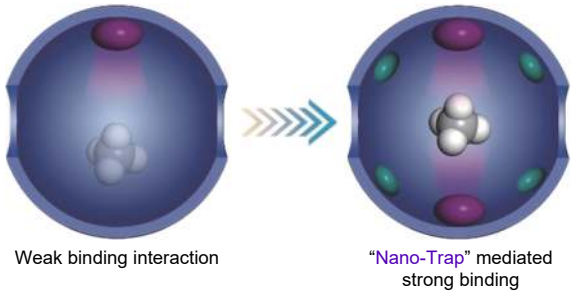

Fig. 19 The comparison of traditional methane adsorbent and nano-trap. The purple and green ellipsoids represent coordinatively unsaturated metal centers and alkyl groups, respectively[159]. Reproduced with permission.

produced in landfills, Matthew et al.[176] used poly vinyl alcohol as a binder for aluminum fumarate, and mixed $MgFe_2O_4$ magnetic nanoparticles with strong heating capacity to prepare aluminum fumarate@$MgFe_2O_4$ magnetic framework composite (MFC), whose methane uptake could reach 18.2 cm^3 g^{-1} at 300 K, 1 bar when the mass fraction of $MgFe_2O_4$ was 1 wt%. A magnetic induction swing adsorption process was adopted to regenerate MFC materials, and the regenerated MFC could reach 100% working capacity within 10 adsorption–desorption cycles.

Snurr et al.[177] performed GCMC simulations of methane adsorption over 4700 MOFs at 270, 298 K and 1, 5.8 and 65 bar. Fig. 20 exhibits an obvious linear relationship between methane uptake and volumetric surface area (VSA)/pore volume at 65 bar (when the pore volume is larger than 1.5 cm^3 g^{-1}, the methane uptake decreases due to the large pore diameter). However, no linear relationship is observed at 1 bar. This is attributed to the fact that methane adsorption

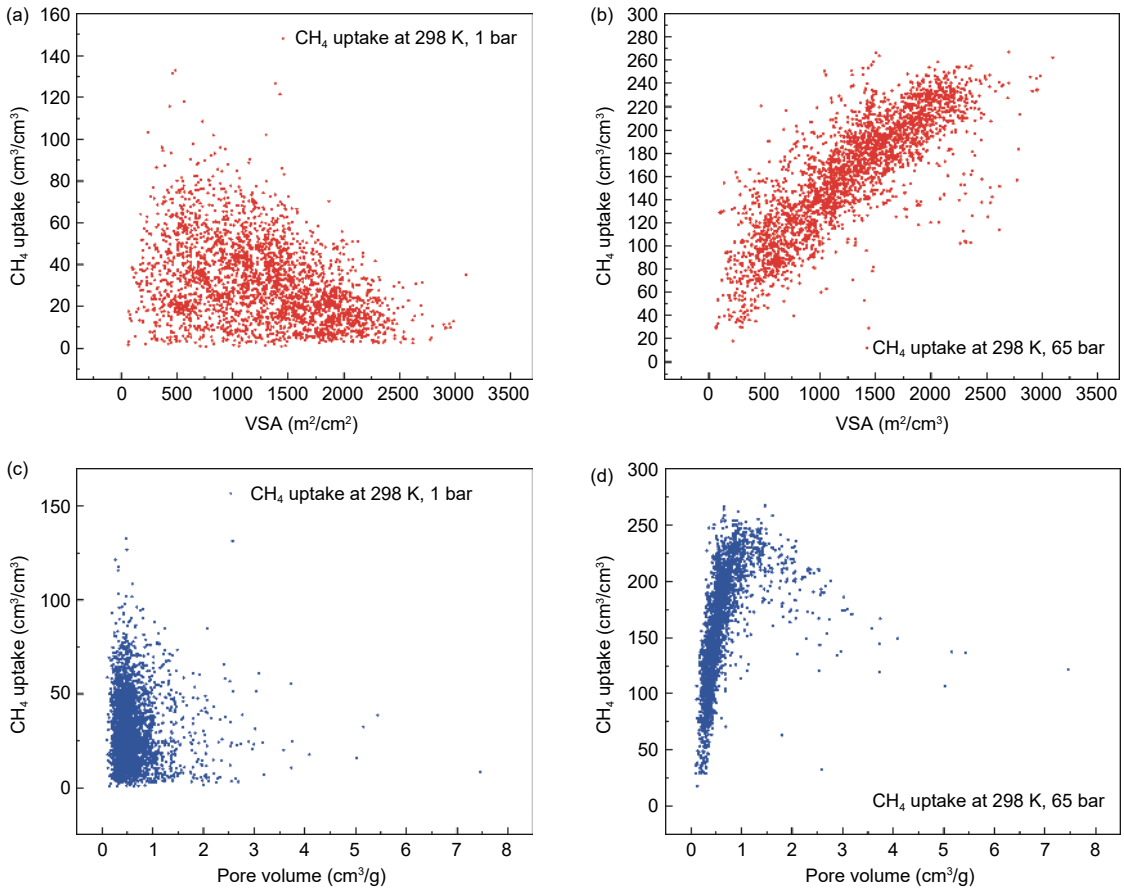

Fig. 20 Relationship between CH_4 uptake and VSA/pore volume at 298 K, 1 bar and 65 bar.

follows BET multi-layer adsorption theory at 65 bar, thus VSA can be used as an intuitive index to characterize the adsorption capacity of MOFs under high pressure. However, the BET theory is only applicable to the case when $0.5 < p/p_0 < 0.35$, and not suitable for adsorption under atmospheric pressure, which indicates that it is more difficult and challenging to design MOFs that capture methane under atmospheric pressure.

5.4 Issues and prospects

Previous research focused on high-pressure storage of methane for use in automobile fuels. However, with increasing attention to environmental issues in recent years, the serious harm of methane as a greenhouse gas has been gradually realized. Owing to the commercial value and resource attributes of methane, physical adsorption has become a methane recovery and emission reduction method with great potential application value. Compared to high-pressure storage of methane, low-pressure conditions are not conducive to methane adsorption. In the past, few scholars conducted in-depth studies on the methane adsorption characteristics of MOFs at low pressures. Therefore, to find an effective way to maximize the advantages of MOFs through optimizing structural design, introducing functional groups, and improving the physical and chemical properties of the surface to enhance the methane uptake at room temperature and atmospheric pressure is the focus of future research. Furthermore, the big data method can also be used as an effective method for structural pre-screening; nonetheless, it still needs more experimental data support, and previous studies have found that it is more difficult to accurately predict the methane uptake under low pressures. Therefore, it is necessary to introduce descriptors capable of characterizing the adsorption characteristics of methane at low pressures. Similarly, recyclability and economy are also important factors to be considered in practical application.

6 Conclusions

As two major low-carbon energy technologies, methane storage and methane capture face the same challenge, that is, the lack of efficient adsorbents. Metal–organic framework (MOF) is a very promising candidate material for adsorbents because of its high porosity, specific surface area, and strong designability. In the aspect of high pressure storage of methane as vehicle fuel, there is no MOFs material that can meet the adsorption targets proposed by DOE on the premise of economy. The author believes that in the structural design of MOFs, the effects of many factors such as material pore volume, open metal sites, and functional groups on the total uptake and deliverable capacity should be considered at the same time. Utilization of flexible MOFs proposed in recent years is a promising method to improve the deliverable capacity. In addition to methane uptake, thermal management strategy, impurity tolerance, recyclability, and cost should be considered in large-scale application. In the aspect of methane capture by MOFs, previous studies focused on the separation performance of methane/impurities; however, the capture of single methane component has been rarely investigated. Without consideration of deliverable capacity, the key to improve the capture capability of methane is how to enhance the interaction between methane and the framework under room atmospheric temperature and pressure through structural optimization, and cyclability and cost are also the main issues to be considered. Moreover, due to the strong designability and existence of wide variety of MOFs materials, the big data analysis method is expected to reveal the key material properties in specific applications by introducing descriptors that describe the structure/properties of materials, so as to guide material design, which is a promising method to realize fast and accurate pre-screening of MOFs in the future.

Acknowledgments

This research was funded by the National Natural Science Foundation of China (51774315, 51704319), the Fundamental Research Funds for the Central Universities (18CX02172A).

References

[1] IEA, Methane from oil & gas-Methane Tracker 2021-Analysis-

IEA, Paris. 2021.01. https://www.iea.org/fuels-and-technologies/methane-abatement.

[2] Cracknell, Roger F. Gordon, Peter Gubbins, Keith E. Influence of pore geometry on the design of microporous materials for methane storage[J]. The Journal of Physical Chemistry, 1993, 97(2): 494-499.

[3] V. C. Menon, S. Komarneni. Porous adsorbents for vehicular natural gas storage: A review[J]. Journal of Porous Materials, 1998, 5(1): 43-58.

[4] Jarad A. Mason, Mike Veenstra, Jeffrey R. Long. Evaluating metal–organic frameworks for natural gas storage[J]. Chemical Science, 2013, 5(1): 32-51.

[5] Mirian Elizabeth Casco, Manuel Martínez-Escandell, Enrique Gadea-Ramos, et al. High-Pressure methane storage in porous materials: are carbon materials in the pole position?[J]. Chemistry of Materials, 2015, 27(3): 959-964.

[6] Wai Soong Loh, Kazi Afzalur Rahman, Anutosh Chakraborty, et al. Improved isotherm data for adsorption of methane on activated carbons[J]. Journal of Chemical & Engineering Data, 2010, 55(8): 2840-2847.

[7] Bin Li, Hui-Min Wen, Wei Zhou, et al. Porous metal-organic frameworks: promising materials for methane storage[J]. Chem, 2016, 1(4): 557-580.

[8] YG Chung, E Haldoupis, BJ Bucior, et al. Advances, updates, and analytics for the computation-ready, experimental metal–organic framework database: CoRE MOF 2019[J]. Journal of Chemical & Engineering Data, 2019, 64(12): 5985-5998.

[9] Furukawa Hiroyasu, Go Yong Bok, Ko Nakeun, et al. Isoreticular expansion of metal-organic frameworks with triangular and square building units and the lowest calculated density for porous crystals[J]. Inorganic chemistry, 2011, 50(18): 9147-9152.

[10] Stephen S. -Y. Chui, Samuel M. -F. Lo, Jonathan P. H. Charmant, et al. A chemically functionalizable nanoporous material $[cu_3(tma)_2(h_2o)_3]_n$[J]. Science, 1999, 283(5405): 1148-1150.

[11] G. Férey, C. Mellot-Draznieks, C. Serre, et al. A chromium terephthalate-based solid with unusually large pore volumes and surface area[J]. Science, 2005, 309(5743): 2040-2042.

[12] Young Kwan Park, Sang Beom Choi, Hyunuk Kim, et al. Titelbild: crystal structure and guest uptake of a mesoporous metal–organic framework containing cages of 3.9 and 4.7 nm in diameter[J]. Angewandte Chemie, 2007, 119(43): 8237-8237.

[13] Yan Yong, Yang Sihai, Blake Alexander J, et al. A mesoporous metal-organic framework constructed from a nanosized C3-symmetric linker and $[Cu_{24}(isophthalate)_{24}]$ cuboctahedra[J]. Chemical communications (Cambridge, England), 2011, 47(36): 9995-9997.

[14] Jie Peng Zhang, Yue Biao Zhang, Jian Bin Lin, et al. ChemInform abstract: metal azolate frameworks: from crystal engineering to functional materials[J]. ChemInform, 2012, 43(16): 1001-1033.

[15] Hideki Hayashi, Adrien P. Côté, Hiroyasu Furukawa, et al. Zeolite a imidazolate frameworks[J]. Nature Materials, 2007, 6(7): 501-506.

[16] Wang Bo, Côté Adrien P, Furukawa Hiroyasu, et al. Colossal cages in zeolitic imidazolate frameworks as selective carbon dioxide reservoirs[J]. Nature, 2008, 453(7192): 207-211.

[17] Banerjee Rahul, Furukawa Hiroyasu, Britt David, et al. Control of pore size and functionality in isoreticular zeolitic imidazolate frameworks and their carbon dioxide selective capture properties[J]. Journal of the American Chemical Society, 2009, 131(11): 3875-3877.

[18] R Banerjee, A Phan, B Wang, et al. High-throughput synthesis of zeolitic imidazolate frameworks and application to CO_2 capture[J]. Science, 2008, 319(5865): 939-943.

[19] Yang Huimin, Zhang Xu, Zhang Guiyang, et al. An alkaline-resistant Ag(i)-anchored pyrazolate-based metal-organic framework for chemical fixation of CO_2[J]. Chemical communications (Cambridge, England), 2018, 54(35): 4469-4472.

[20] Putu Doddy Sutrisna, Nicholaus Prasetya, Nurul Faiqotul Himma, et al. A mini-review and recent outlooks on the synthesis and applications of zeolite imidazolate framework-8(ZIF-8) membranes on polymeric substrate[J]. Journal of Chemical Technology & Biotechnology, 2020, 95(11): 2767-2774.

[21] Yue-Biao Zhang, Hao-Long Zhou, Rui-Biao Lin, et al. Geometry analysis and systematic synthesis of highly porous isoreticular frameworks with a unique topology[J]. Nature Communications, 2012, 3(1): 642.

[22] T J Prior, D Bradshaw, S J Teat, et al. Designed layer assembly: a three-dimensional framework with 74% extra-framework volume by connection of infinite two-dimensional sheets[J]. Chemical Communications, 2003, 4(4): 500-501.

[23] Kitaura, R., Iwahori, F., Matsuda, R., et al. Rational design and crystal structure determination of a 3-D Metal-organic jungle-gym-like open framework[J]. Inorganic Chemistry, 2004, 43(21): 6522-6524.

[24] Yating Zhang, Peng Wang, Juan Yang, et al. Fabrication of core-shell nanohybrid derived from iron-based metal-organic framework grappled on nitrogen-doped graphene for oxygen reduction reaction[J]. Chemical Engineering Journal, 2020, 401: 126001.

[25] Zhang Yating, Wang Peng, Yang Juan, et al. Decorating ZIF-67-derived cobalt-nitrogen doped carbon nanocapsules on 3D carbon frameworks for efficient oxygen reduction and oxygen evolution[J]. Carbon, 2021, 177: 344-356.

[26] Patrick J. Beldon, Dr. László Fábián, Dr. Robin S. Stein, et al. Rapid room-temperature synthesis of zeolitic imidazolate frameworks by using mechanochemistry[J]. Angewandte Chemie International Edition, 2010, 49(50): 9640-9643.

[27] Crawford Deborah, Casaban José, Haydon Robert, et al. Synthesis by extrusion: continuous, large-scale preparation of MOFs using little or no solvent[J]. Chemical science, 2015, 6(3): 1645-1649.

[28] Patricia Silva, Sergio M. F. Vilela, Joao P. C. Tome, et al. ChemInform abstract: multifunctional metal-organic frameworks: from academia to industrial applications[J]. ChemInform, 2015, 46(46): 6774-6803.

[29] Albuquerque G H, Herman G S. Chemically modulated

microwave-assisted synthesis of MOF-74(Ni) and preparation of MOF-matrix based membranes for removal of metal ions from aqueous media[J]. Crystal Growth & Design, 2016, 17(1): 156-162.

[30] Dreischarf Anna C, Lammert Martin, Stock Norbert, et al. Green synthesis of Zr-CAU-28: structure and properties of the first Zr-MOF based on 2, 5-furandicarboxylic acid[J]. Inorganic chemistry, 2017, 56(4): 2270-2277.

[31] Xu Lan Lan, Wang Song, Liu Yu xia, et al. Advance on research and application of MOF prepared by MW method[J]. New Chemical Materials, 2019, 47(04): 1-5.

[32] Jhung S H, Lee J H, Chang J S. Microwave synthesis of a nanoporous hybrid material, chromium trimesate[J]. Bulletin of the Korean Chemical Society, 2005, 26(6): 880-883.

[33] Nesa Esmaeilian Tari, Azadeh Tadjarodi, Javad Tamnanloo, et al. Facile and fast, one pot microwave synthesis of metal organic framework copper terephthalate and study CO_2 and CH_4 adsorption on it[J]. Journal of Porous Materials, 2015, 22(5): 1161-1169.

[34] Hye-Young Cho, Da-Ae Yang, Jun Kim, et al. CO_2 adsorption and catalytic application of Co-MOF-74 synthesized by microwave heating[J]. Catalysis Today, 2012, 185(1): 35-40.

[35] Palomino Cabello Carlos, Arean Carlos Otero, Parra José B, et al. A rapid microwave-assisted synthesis of a sodium-cadmium metal-organic framework having improved performance as a CO_2 adsorbent for CCS[J]. Dalton transactions (Cambridge, England: 2003), 2015, 44(21): 9955-9963.

[36] Pradip Sarawade, Hua Tan, Vivek Polshettiwar. Shape-and morphology-controlled sustainable synthesis of Cu, Co, and in metal organic frameworks with high CO_2 capture capacity[J]. ACS Sustainable Chemistry & Engineering, 2012, 1(1): 66-74.

[37] Bao Zongbi, Yu Liang, Ren Qilong, et al. Adsorption of CO_2 and CH_4 on a magnesium-based metal organic framework[J]. Journal of colloid and interface science, 2011, 353(2): 549-556.

[38] Chandan Dey, Tanay Kundu, Bishnu P. Biswal, et al. Crystalline metal-organic frameworks (MOFs): synthesis, structure and function[J]. Acta Crystallographica Section B, 2014, 70(1): 3-10.

[39] U. Mueller, M. Schubert, F. Teich, et al. Metal-organic frameworks —prospective industrial applications[J]. Journal of Materials Chemistry, 2006, 16(23): 626-636.

[40] Tom R. C. Van Assche, Gert Desmet, Rob Ameloot, et al. Electrochemical synthesis of thin hkust-1 layers on copper mesh[J]. Microporous and Mesoporous Materials, 2012: 209-213.

[41] Stassen I, Styles M, Assche T V, et al. Electrochemical film deposition of the zirconium metal–organic framework UiO-66 and application in a miniaturized sorbent trap[J]. Chemistry of Materials, 2015, 27(5): 379-391.

[42] Christos Vaitsis, Georgia Sourkouni, Christos Argirusis. Metal organic frameworks (MOFs) and ultrasound: a review[J]. Ultrasonics Sonochemistry, 2019: 52.

[43] Suslick K S, Hammerton D A, Cline R E. Sonochemical hot spot[J]. Journal of the American Chemical Society, 1986, 89(18): 5641-5642.

[44] Suslick K S. Sonochemistry[J]. Cheminform, 1990, 247(4949): 1439-1445.

[45] Qiu Ling-Guang, Li Zong-Qun, Wu Yun, et al. Facile synthesis of nanocrystals of a microporous metal-organic framework by an ultrasonic method and selective sensing of organoamines[J]. Chemical communications (Cambridge, England), 2008(31): 3642-3644.

[46] Son Won-Jin, Kim Jun, Kim Jaheon, et al. Sonochemical synthesis of MOF-5[J]. Chemical communications (Cambridge, England), 2008(47): 6336-6338.

[47] Zong-Qun Li, Ling-Guang Qiu, Wei Wang, et al. Fabrication of nanosheets of a fluorescent metal-organic framework $[zn(bdc)(h_2o)]_n$(bdc-1,4-benzenedicarboxylate): ultrasonic synthesis and sensing of ethylamine[J]. Inorganic Chemistry Communications, 2008, 11(11): 1375-1377.

[48] Cohen Seth M. Postsynthetic methods for the functionalization of metal-organic frameworks[J]. Chemical reviews, 2012, 112(2): 970-1000.

[49] Cai Y, Zhang Y, Huang Y, et al. Impact of alkyl-functionalized btc on properties of copper-based metal-organic frameworks[J]. Crystal Growth & Design, 2012, 12(7): 3709-3713.

[50] Yichao Lin, Chunglong Kong, Qiuju Zhang, et al. Metal-organic frameworks for carbon dioxide capture and methane storage[J]. Advanced Energy Materials, 2017, 7(4): 1601296.

[51] Christopher E. Wilmer, Michael Leaf, Chang Yeon Lee, et al. Large-scale screening of hypothetical metal-organic frameworks[J]. Nature Chemistry, 2012, 4(2): 83-89.

[52] Martin Richard L, Simon Cory M, Smit Berend, et al. In silico design of porous polymer networks: high-throughput screening for methane storage materials[J]. Journal of the American Chemical Society, 2014, 136(13): 5006-5022.

[53] Simon C M, Kim J, Gomez-Gualdron D A, et al. The materials genome in action: identifying the performance limits for methane storage[J]. Energy & Environmental Science, 2015, 8(4): 1190-1199.

[54] Simon C M, Kim J, Lin L C, et al. Optimizing nanoporous materials for gas storage[J]. Physical Chemistry Chemical Physics Pccp, 2014, 16(12): 5499-5513.

[55] YJ Colón, Fairen-Jimenez D, Wilmer C E, et al. High-throughput screening of porous crystalline materials for hydrogen storage capacity near room temperature[J]. The Journal of Physical Chemistry C, 2016, 118(10): 5383-5389.

[56] Bobbitt N S, Chen J, Snurr R Q. High-throughput screening of metal-organic frameworks for hydrogen storage at cryogenic temperature[J]. Journal of Physical Chemistry C, 2016, 120(48): 27328-27341.

[57] Gomez-Gualdron D, YJ Colón, Zhang X, et al. Evaluating topologically diverse metal–organic frameworks for cryo-adsorbed hydrogen storage[J]. Energy & Environmental Science, 2016, 9(10): 3279-3289.

[58] Han S, Huang Y, Watanabe T, et al. High-throughput screening of metal-organic frameworks for CO_2 separation[J]. ACS Combinatorial Science, 2012, 14(4): 263-267.

[59] Yongchul G. Chung, Diego A. Gómez-Gualdrón, Peng Li, et al. In silico discovery of metal-organic frameworks for precombustion CO_2 capture using a genetic algorithm[J]. Science Advances, 2016, 2(10): e1600909-e1600909.

[60] Simon C M, Mercado R, Schnell S K, et al. What are the best materials to separate a xenon/krypton mixture?[J]. Chemistry of Materials, 2015, 27(12): 4459-4475.

[61] Curtarolo S, Hart G L W, Nardelli M B, et al. The high-throughput highway to computational materials design[J]. Nature Materials, 2013, 12(3): 191-201.

[62] Canepa P, Arter C A, Conwill E M, et al. High-throughput screening of small-molecule adsorption in MOF[J]. Journal of Materials Chemistry A, 2013, 1: 13597-13604.

[63] Wollmann Philipp, Leistner Matthias, Stoeck Ulrich, et al. High-throughput screening: speeding up porous materials discovery[J]. Chemical communications (Cambridge, England), 2011, 47(18): 5151-5153.

[64] Gee J A, Zhang K, Bhattacharyya S, et al. Computational identification and experimental evaluationof metal –organic frameworks for xylene enrichment[J]. Journal of Physical Chemistry C, 2016, 120(22): 12075-12082.

[65] Demir H, Walton K S, Sholl D S. Computational screening of functionalized UiO-66 materials for selective contaminant removal from air[J]. The Journal of Physical Chemistry C, 2017, 121(37): 20396-20406.

[66] Christopher, E, WHmer, et al. Structure-property relationships of porous materials for carbon dioxide separation and capture[J]. Energy & environmental science: EES, 2012, 5(12): 9849-9856.

[67] Fernandez M, Barnard A S. Geometrical properties can predict CO_2 and N_2 adsorption performance of metal-organic frameworks (MOFs) at low pressure[J]. acs combinatorial science, 2016, 18(5): 243-252.

[68] Fernandez M, Woo T K, Wilmer C E, et al. Large-scale quantitative structure –property relationship (qspr) analysis of methane storage in metal–organic frameworks[J]. The Journal of Physical Chemistry C, 2013, 117(15): 7681-7689.

[69] Braun E, AF Zurhelle, Thijssen W, et al. High-throughput computational screening of nanoporous adsorbents for CO_2 capture from natural gas[J]. Molecular Systems Design & Engineering, 2016, 1: 175-188.

[70] Pardakhti Maryam, Moharreri Ehsan, Wanik David, et al. Machine learning using combined structural and chemical descriptors for prediction of methane adsorption performance of metal organic frameworks (MOFs)[J]. ACS Combinatorial Science, 2017, 19(10): 640-645.

[71] Fanourgakis G S, K Gkagkas, Tylianakis E, et al. A generic machine learning algorithm for the prediction of gas adsorption in nanoporous materials[J]. The Journal of Physical Chemistry C, 2019, 123(28): 6080-6087.

[72] Hui W, Simmons J, Yun L, et al. Metal-organic frameworks with exceptionally high methane uptake: where and how is methane stored?[J]. Chemistry, 2010, 16(17): 5205-5214.

[73] Tsivion E, Mason J A, Gonzalez M, et al. A computational study of CH_4 storage in porous framework materials with metalated linkers: connecting the atomistic character of CH_4 binding sites to usable capacity[J]. Chem Sci, 2016, 7(7): 4503-4518.

[74] Czaja A, Trukhan N, Muller U. Industrial applications of metal-organic frameworks[J]. Chemical Society Reviews, 2009, 38(5): 1284-1293.

[75] He Y, Zhou W, Qian G, et al. Methane storage in metal–organic frameworks[J]. Chemical Society Reviews, 2014, 43(16): 5657-5678.

[76] Kondo M, Yoshitomi T, Matsuzaka H, et al. Three-dimensional framework with channeling cavities for small molecules: $\{[m_2(4,4\text{ '-bpy})_3(no_3)_4]\cdot xh_2O_n$ (m co,ni,zn)[J]. Angewandte Chemie International Edition in English, 1997, 36(16): 1725-1727.

[77] Li H L, Eddaoudi M M, O'Keeffe M, et al. Design and synthesis of an exceptionally stable and highly porous metal-organic framework[J]. Nature, 1999, 402(6759): 276-279.

[78] Eddaoudi, M. Systematic design of pore size and functionality in isoreticular MOFs and their application in methane storage[J]. Science, 2002, 295(5554): 469-472.

[79] Chae H K, Siberio-Perez D Y, Kim J, et al. A route to high surface area, porosity and inclusion of large molecules in crystals[J]. Nature, 2004, 427(6974): 523-527.

[80] Furukawa Hiroyasu, Ko Nakeun, Go Yong Bok, et al. Ultrahigh porosity in metal-organic frameworks[J]. Science (New York, N. Y.), 2010, 329(5990): 424-428.

[81] He Y, Wei Z, Yildirim T, et al. A series of metal –organic frameworks with high methane uptake and an empirical equation for predicting methane storage capacity[J]. Energy & Environmental Science, 2013, 6(9): 2735-2744.

[82] Li B, Wen H M, Wang H, et al. A porous metal-organic framework with dynamic pyrimidine groups exhibiting record high methane storage working capacity[J]. Journal of the American Chemical Society, 2014, 136(17): 6207-6210.

[83] Alezi D, Belmabkhout Y, Suyetin M, et al. MOF crystal chemistry paving the way to gas storage needs: aluminum-based soc-MOF for CH_4, O_2, and CO_2 storage[J]. Journal of the American Chemical Society, 2015, 137(41): 13308-13318.

[84] F Gándara, Furukawa H, Lee S, et al. High methane storage capacity in aluminum metal-organic frameworks[J]. Journal of the American Chemical Society, 2014, 136(14): 5271-5274.

[85] Rosi N L, Kim J, Eddaoudi M, et al. Rod packings and metal-organic frameworks constructed from rod-shaped secondary building units[J]. Journal of the American Chemical Society, 2005, 127(5): 1504-1518.

[86] Ma S, Sun D, Simmons J M, et al. Metal-organic framework from an anthracene derivative containing nanoscopic cages exhibiting high methane uptake[J]. Journal of the American Chemical Society, 2008, 130(3): 1012-1016.

[87] Zheng B, D Tian, Zhang L, et al. Investigation of methane adsorption in strained IRMOF-1[J]. The Journal of Physical Chemistry C, 2019, 123(40): 24592-24597.

[88] Kong G, Han Z, He Y, et al. Expanded organic building units for

the construction of highly porous metal –organic frameworks (pages 14886–14894)[J]. Hokkai-Gakuen University, The Journal of Economics, 2006, 54(44): 35-52.

[89] Purewal J J, Liu D, Yang J, et al. Increased volumetric hydrogen uptake of MOF-5 by powder densification[J]. International Journal of Hydrogen Energy, 2012, 37(3): 2723-2727.

[90] Hui W, Yildirim T, Zhou W. Exceptional mechanical stability of highly porous zirconium metal–organic framework uio-66 and its important implications[J]. Journal of Physical Chemistry Letters, 2013, 4(6): 925-930.

[91] Yang P, Krungleviciute V, Eryazici I, et al. Methane storage in metal-organic frameworks: current records, surprise findings, and challenges[J]. Journal of the American Chemical Society, 2013, 135(32): 11887-11894.

[92] Tian T, Zeng Z, Vulpe D, et al. A sol –gel monolithic metal –organic framework with enhanced methane uptake[J]. Nature Materials, 2018, 17(2): 174-179.

[93] Jeong N C, Samanta B, Chang Y L, et al. Coordination-chemistry control of proton conductivity in the iconic metal-organic framework material hkust-1[J]. Journal of the American Chemical Society, 2012, 134(1): 51-54.

[94] HuiMin Wen, Bin Li, Libo Li, et al. A metal-organic framework with optimized porosity and functional sites for high gravimetric and volumetric methane storage working capacities[J]. Advanced Materials, 2018, 30(16): 1704792-1704792.

[95] Jiang J, Furukawa H, Zhang Y B, et al. high methane storage working capacity in metal-organic frameworks with acrylate links[J]. Journal of the American Chemical Society, 2016, 138(32): 10244-10251.

[96] Mason J A, Oktawiec J, Taylor M K, et al. Methane storage in flexible metal-organic frameworks with intrinsic thermal management[J]. Nature, 2015, 527(7578): 357-361.

[97] Jiao-Min, Lin, ChunTing, et al. A Metal-organic framework with a pore size/shape suitable for strong binding and close packing of methane[J]. Angewandte Chemie, 2015, 55(15): 4674-4678.

[98] Yang P, Srinivas G, Wilmer C E, et al. Simultaneously high gravimetric and volumetric methane uptake characteristics of the metal –organic framework NU-111[J]. Chemical Communications, 2013, 49(29): 2992-2994.

[99] Chen Z, Li P, Anderson R, et al. Balancing volumetric and gravimetric uptake in highly porous materials for clean energy[J]. Science, 2020, 368(6488): 297-303.

[100] Mason J A, Veenstra M, Long J R. ChemInform abstract: evaluating metal-organic frameworks for natural gas storage[J]. Cheminform, 2014, 45(16): 32-51.

[101] H Li, Li L, Lin R B, et al. Porous Metal-organic frameworks for gas storage and separation: status and challenges[J]. EnergyChem, 2019, 1(1): 10006-10006.

[102] Chen Cheng-Xia, Wei Zhang-Wen, Jiang Ji-Jun, et al. Dynamic spacer installation for multirole metal-organic frameworks: a new direction toward multifunctional MOFs achieving ultrahigh methane storage working capacity[J]. Journal of the American Chemical Society, 2017, 139(17): 6034-6037.

[103] Yan Y, Kolokolov D I, Silva I D, et al. Porous metal–organic polyhedral frameworks with optimal molecular dynamics and pore geometry for methane storage[J]. Journal of the American Chemical Society, 2017, 139(38): 13349-13360.

[104] Bourrelly S, Llewellyn P L, Serre C, et al. Different adsorption behaviors of methane and carbon dioxide in the isotypic nanoporous metal terephthalates MIL-53 and MIL-47[J]. Journal of the American Chemical Society, 2005, 127(39): 13519-13521.

[105] Llewellyn Philip L, Bourrelly Sandrine, Serre Christian, et al. High uptakes of CO_2 and CH_4 in mesoporous metal organic frameworks MIL-100 and MIL-101[J]. Langmuir, 2008, 24(14): 7245-7250.

[106] Hong D Y, Hwang Y K, Serre C, et al. Porous chromium terephthalate MIL - 101 with coordinatively unsaturated sites: surface functionalization, encapsulation, sorption and catalysis[J]. Advanced Functional Materials, 2010, 19(10): 1537-1552.

[107] Rosi, N. L. Hydrogen storage in microporous metal-organic frameworks[J]. Science, 2003, 300(5622): 1127-1129.

[108] Zhou W, Wu H, Hartman M R, et al. Hydrogen and methane adsorption in metal-organic frameworks: A high-pressure volumetric study[J]. The Journal of Physical Chemistry C, 2007, 111(44): 16131-16137.

[109] J Bai, Zhang M, Zhou W, et al. Fine tuning of MOF - 505 analogues to reduce low-pressure methane uptake and enhance methane working capacity[J]. Angewandte Chemie, 2017, 129(38): 11584-11588.

[110] R. D. Kennedy, V. Krungleviciute, D. J. Clingerman. Carborane-based metal-organic framework with high methane and hydrogen storage capacities[J]. Chemistry of Materials, 2013, 25(17): 3539-3543.

[111] Dan Z, Yuan D, Sun D, et al. Stabilization of metal-organic frameworks with high surface areas by the incorporation of mesocavities with microwindows[J]. Journal of the American Chemical Society, 2009, 131(26): 9186-9188.

[112] D Yuan, Dan Z, D Sun, et al. An isoreticular series of metal–organic frameworks with dendritic hexacarboxylate ligands and exceptionally high gas-uptake capacity[J]. Angewandte Chemie International Edition, 2010, 49(31): 5357-5361.

[113] Bin Li, Huimin Wen, Hailong Wang, et al. Porous metal-organic frameworks with Lewis basic nitrogen sites for high-capacity methane storage[J]. Energy & Environmental Science, 2015, 8(8): 2504-2511.

[114] Duan X, Wu C, Xiang S, et al. Novel microporous metal–organic framework exhibiting high acetylene and methane storage capacities[J]. Inorganic Chemistry, 2015, 54(9): 4377-4381.

[115] C. Özgen Karacan, Felicia A. Ruiz, Michael Cotè, et al. Coal mine methane: A review of capture and utilization practices with benefits to mining safety and to greenhouse gas reduction[J]. International Journal of Coal Geology, 2011, 86(2-3): 121-156.

[116] Bongaarts J. Intergovernmental panel on climate change special report on global warming of 1.5°C switzerland: IPCC, 2018[J]. Population and Development Review, 2019, 45(1): 251-252.

[117] Ramón A. Alvarez, Daniel Zavala-Araiza, David R. Lyon, et al.

Assessment of methane emissions from the U. S. oil and gas supply chain[J]. Science, 2018, 361(6398): 186-188.

[118] IEA, Methane emissions from oil and gas, comparison of IEA and other estimates[Z]. IEA, Paris. 2020.08. 30 https://www.iea.org/data-and-statistics/charts/methane-emissions-from-oil-and-gas-comparison-of-iea-and-other-estimates.

[119] IEA, Oil and gas sector methane emissions, historical and in the sustainable development scenario, 2000-2030[Z], IEA, Paris. https://www.iea.org/data-and-statistics/charts/oil-and-gas-sector-methane-emissions-historical-and-in-the-sustainable-development-scenario-2000-2030

[120] Melse R, Aw V D W. Biofiltration for mitigation of methane emission from animal husbandry[J]. Environmental Science & Technology, 2005, 39(14): 5460-5468.

[121] Girard M, Ramirez A A, Buelna G, et al. Biofiltration of methane at low concentrations representative of the piggery industry-Influence of the methane and nitrogen concentrations[J]. Chemical Engineering Journal, 2011, 168(1): 151-158.

[122] Stuart, A, Dever, et al. Passive drainage and biofiltration of landfill gas: results of australian field trial[J]. Waste Management, 2011, 31(5): 1029-1048.

[123] Gebert J, Groengroeft A. Performance of a passively vented field-scale biofilter for the microbial oxidation of landfill methane[J]. Waste Manag, 2006, 26(4): 399-407.

[124] Nikiema J, Brzezinski R, Heitz M. Elimination of methane generated from landfills by biofiltration: a review[J]. Reviews in Environmental Science & Bio/technology, 2007, 6(4): 261-284.

[125] Berger J, Fornes L V, Ott C. Methane oxidation in a landfill cover with capillary barrier[J]. Waste Manag, 2005, 25(4): 369-373.

[126] Du P C, Strauss J M, Emt S, et al. Empirical model for methane oxidation using a composted pine bark biofilter[J]. Fuel, 2003, 82(11): 1359-1365.

[127] Climate and Clean Air Coalition. CCAC O&G methane partnership: technical guidance document[R]. Paris, France, 2017.

[128] Shindell D, Fuglestvedt J S, Collins W J. The social cost of methane: theory and applications[J]. Faraday Discussions, 2017, 200: 429-451.

[129] Chaffee A L, Knowles G P, Liang Z, et al. CO capture by adsorption: Materials and process development[J]. international journal of greenhouse gas control, 2007, 1(1): 11-188.

[130] Mcdonald T M, Lee W R, Mason J A, et al. Capture of carbon dioxide from air and flue gas in the alkylamine-appended metal-organic framework mmen-Mg2(dobpdc)[J]. Journal of the American Chemical Society, 2012, 134(16): 7056-7065.

[131] Moon S H, Shim J W. A novel process for CO_2/CH_4 gas separation on activated carbon fibers--electric swing adsorption[J]. J Colloid Interface, 2006, 298(2): 523-528.

[132] Plaza M G, S García, Rubiera F, et al. Post-combustion CO_2 capture with a commercial activated carbon: Comparison of different regeneration strategies[J]. Chemical Engineering Journal, 2010, 163(1–2): 41-47.

[133] Kim J, Maiti A, Lin L C, et al. New materials for methane capture from dilute and medium-concentration sources[J]. Nature Communications, 2013, 4: 1694.

[134] Myrsini K. Antoniou, Evmorfia K. Diamanti, Apostolos Enotiadis, et al. Methane storage in zeolite-like carbon materials[J]. Microporous and Mesoporous Materials, 2014, 188: 16-22.

[135] Bae J S, Su S, Yu X X. Enrichment of ventilation air methane (VAM) with carbon fiber composites[J]. Environmental Science & Technology, 2014, 48(10): 6043-6049.

[136] Beckner M, Dailly A. A pilot study of activated carbon and metal –organic frameworks for methane storage[J]. Applied Energy, 2016, 162(JAN. 15): 506-514.

[137] J Sreńscek-Nazzal, W Kamińska, Michalkiewicz B, et al. Production, characterization and methane storage potential of KOH-activated carbon from sugarcane molasses[J]. Industrial Crops & Products, 2013, 47: 153-159.

[138] Ali, Bakhtyari, Masoud, et al. Pure and binary adsorption equilibria of methane and nitrogen on zeolite 5A[J]. Journal of Chemical & Engineering Data, 2014, 59(3): 626-639.

[139] Makal T A, Li J R, Lu W, et al. Methane storage in advanced porous materials[J]. Chemical Society Reviews, 2012, 41(23): 7761-7779.

[140] Baudot A. CH_4/N_2 Separation[M]. 2016.

[141] Kuznicki S M, Bell V A, Nair S, et al. A titanosilicate molecular sieve with adjustable pores for size-selective adsorption of molecules[J]. Nature, 2001, 412(6856): 720-724.

[142] Yang, Ralph T. Adsorbents: fundamentals and applications[J]. Belgeler Com, 2003, 2004: xii,404.

[143] Jayaraman A, Hernandez-Maldonado A J, Yang R T, et al. Clinoptilolites for nitrogen/methane separation[J]. Chemical Engineering Science, 2004, 59(12): 2407-2417.

[144] Liu, Xiao-Wei, Hu, Jiang-Liang, Sun, Tian-Jun, et al. Template-based synthesis of a formate metal-organic framework/activated carbon fiber composite for high-performance methane adsorptive separation[J]. Chemistry-An Asian Journal, 2016, 11(21): 3014-3017.

[145] Yang, R. Principle and application of adsorbent [M]. Higher Education Press, 2010..

[146] Rege S, Yang R. A simple parameter for selecting an adsorbent for gas separation by pressure swing adsorption[J]. Separation Science & Technology, 2001, 36(15): 3355-3365.

[147] Bae Y S, Snurr R Q. Development and evaluation of porous materials for carbon dioxide separation and capture[J]. Cheminform, 2011, 50(49): 11586-11596.

[148] Li Q, Ruan M, Lin B, et al. Molecular simulation study of metal organic frameworks for methane capture from low-concentration coal mine methane gas[J]. Journal of Porous Materials, 2016, 23(1): 107-122.

[149] Sumer Z, Keskin S. Adsorption- and membrane-based CH_4/N_2 separation performances of MOFs[J]. Industrial & Engineering Chemistry Research, 2017, 56(30): 8713-8722.

[150] Liu X, Guo Y, Tao A, et al. "Explosive" synthesis of metal-formate frameworks for methane capture: an experimental and computational study[J]. Chem Commun, 2017, 53(83): 11437-11440.

[151] Liu X W, Gu Y, Sun T J, et al. Water resistant and flexible MOF materials for highly-efficient separation of methane from nitrogen[J]. Industrial & Engineering Chemistry Research, 2019, 58(44): 20392-20400.

[152] Daofei Lv, Ying Wu, Jiayu Chen, et al. Improving CH_4/N_2 selectivity within isomeric Al-based MOFs for the highly selective capture of coal-mine methane[J]. AIChE Journal, 2020, 66(9): e16287-e16287.

[153] Liangying Li, Lifeng Yang, Jiawei Wang, et al. Highly efficient separation of methane from nitrogen on a squarate-based metal-organic framework[J]. AIChE Journal, 2018, 64(10): 3681-3689.

[154] Li L, Yang J, Li J, et al. Separation of CO_2/CH_4 and CH_4/N_2 mixtures by M/DOBDC: A detailed dynamic comparison with MIL-100(Cr) and activated carbon[J]. Microporous & Mesoporous Materials, 2014, 198: 236-246.

[155] Saha D, Bao Z, Jia F, et al. Adsorption of CO_2, CH_4, N_2O, and N_2 on MOF-5, MOF-177, and zeolite 5A[J]. Environmental Science & Technology, 2017, 44(5): 1820-1826.

[156] Ren X, Sun T, Hu J, et al. Highly enhanced selectivity for the separation of CH_4 over N_2 on two ultra-microporous frameworks with multiple coordination modes[J]. Microporous & Mesoporous Materials, 2014, 186: 137-145.

[157] Lv D, Shi R, Chen Y, et al. Selective adsorptive separation of CO_2/CH_4 and CO_2/N_2 by a water resistant zirconium-porphyrin metal-organic framework[J]. Industrial & Engineering Chemistry Research, 2018, 57(36): 12215-12224.

[158] David E. Jaramillo, Douglas A. Reed, Henry Z. H. Jiang, et al. Selective nitrogen adsorption via backbonding in a metal-organic framework with exposed vanadium sites[J]. Nature Materials, 2020, 19(5): 517-521.

[159] Niu Z, Cui X, Pham T, et al. A metal-organic framework based methane nano-trap for the capture of coal-mine methane[J]. Angewandte Chemie International Edition, 2019, 58(30): 10138-10141.

[160] Chang M, Zhao Y, Yang Q, et al. Microporous metal–organic frameworks with hydrophilic and hydrophobic pores for efficient separation of CH_4/N_2 mixture[J]. Acs Omega, 2019, 4(11): 14511-14516.

[161] Chang M, Zhao Y, Liu D, et al. Methane-trapping metal–organic frameworks with an aliphatic ligand for efficient CH_4/N_2 separation[J]. Sustainable Energy & Fuels, 2019, 4(1): 138-142.

[162] N. Tippayawong, P. Thanompongchart. Biogas quality upgrade by simultaneous removal of CO_2 and H_2S in a packed column reactor[J]. Energy, 2010, 35(12): 4531-4535.

[163] Gomez L F, Zacharia R, P Bénard, et al. Multicomponent adsorption of biogas compositions containing CO_2, CH_4 and N_2 on Maxsorb and Cu-BTC using extended Langmuir and Doong–Yang models[J]. Adsorption, 2015, 21(5): 433-443.

[164] Pal A, Chand S, Das M C. A water-stable twofold interpenetrating microporous MOF for selective CO_2 adsorption and separation[J]. Inorganic Chemistry, 2017, 56(22): 13991-13997.

[165] Simone, Cavenati, Carlos, et al. Metal organic framework adsorbent for biogas upgrading[J]. Industrial & Engineering Chemistry Research, 2008, 47(16): 6333-6335.

[166] Alexandre F. P. Ferreira, Ana Mafalda Ribeiro, Seda Kulaç, et al. Methane purification by adsorptive processes on MIL-53(Al)[J]. Chemical Engineering Science, 2015, 124: 79-95.

[167] Xiang S, He Y, Zhang Z, et al. Microporous metal-organic framework with potential for carbon dioxide capture at ambient conditions[J]. Nature Communications, 2012, 3: 954.

[168] Caskey S R, Wong-Foy A G, Matzger A J. Dramatic tuning of carbon dioxide uptake via metal substitution in a coordination polymer with cylindrical pores[J]. Journal of the American Chemical Society, 2008, 130(33): 10870-10871.

[169] Chowdhury P, Mekala S, Dreisbach F, et al. Adsorption of CO, CO_2 and CH_4 on Cu-BTC and MIL-101 metal organic frameworks: Effect of open metal sites and adsorbate polarity[J]. Microporous & Mesoporous Materials, 2012, 152(none): 246-252.

[170] Nugent P, Belmabkhout Y, Burd S D, et al. Porous materials with optimal adsorption thermodynamics and kinetics for CO_2 separation[J]. Nature, 2013, 495(7439): 80-84.

[171] Krishna R, Baten J. In silico screening of metal-organic frameworks in separation applications[J]. Physical Chemistry Chemical Physics Pccp, 2011, 13: 10593-10616.

[172] Altintas C, Keskin S. Molecular simulations of MOF membranes and performance predictions of MOF/polymer mixed matrix membranes for CO_2/CH_4 separations[J]. ACS AuthorChoice, 2019, 7(2): 2739-2750.

[173] Hongliang, Huang, Wenjuan, et al. Understanding the effect of trace amount of water on CO_2 capture in natural gas upgrading in metal –organic frameworks: a molecular simulation study[J]. Industrial & Engineering Chemistry Research, 2012, 51(30): 10031-10038.

[174] Demir H, Cramer C J, Siepmann J I. Computational screening of metal–organic frameworks for biogas purification[J]. Molecular Systems Design & Engineering, 2019, 4: 1125-1135.

[175] J Rogacka, A Seremak, A Luna-Triguero. High-throughput screening of metal-Organic frameworks for CO_2 and CH_4 separation in the presence of water[J]. Chemical Engineering Journal, 2020, 403: 126392.

[176] Sadiq M M, M Rubio-Martínez, Zadehahmadi F, et al. Magnetic framework composites for low concentration methane capture[J]. Industrial & Engineering Chemistry Research, 2018, 57(18): 6040-6047.

[177] Yongchul Chung, Jeffrey Camp, Maciej Haranczyk, et al. Computation-ready, experimental metal –organic frameworks: a tool to enable high-throughput screening of nanoporous crystals[J]. Chemistry of Materials, 2014, 26(21): 6185-6192.

多孔金属有机框架材料在甲烷存储与捕集中的研究进展及挑战

李东泽，陈 雷*，刘 刚*，袁子云，李秉繁，张 旭，魏甲强

（中国石油大学（华东）山东省油气储运安全省级重点实验室，山东 青岛 266580）

摘 要： 在全球向可持续低碳经济转型的过程中，作为两大低碳能源技术，甲烷储存和甲烷捕集都面临着同样的挑战，即缺乏高效的吸附剂。MOFs（metal-organic frameworks）材料具有极高的比表面积、孔隙率和可调节的孔隙结构，在气体吸附储存领域拥有极大的潜在应用价值。本文首先介绍了 MOFs 的结构设计和合成方法，综述并强调了 MOFs 材料在 CH_4 储存与捕集方面的研究进展及面临的问题。在 CH_4 高压储存方面，从体积吸附量和质量吸附量两个目标出发，介绍了目前 MOFs 材料储存 CH_4 的研究现状；在 CH_4 常压捕集方面，重点强调了 CH_4/N_2 和 CO_2/CH_4 分离技术和 CH_4 捕集技术。最后，对利用 MOFs 材料实现高效 CH_4 储存和捕集存在的问题和挑战进行了分析和展望。

关键词： 金属有机框架；甲烷；吸附；储存；捕集

文章编号： 1007-8827(2021)03-0468-29 **中图分类号：** TQ519 **文献标识码：** A

基金项目: 国家自然科学基金项目（51774315, 51704319），中央高校基本科研业务费专项资金（18CX02172A）.

通讯作者: 陈 雷，副教授. E-mail: leo@upc.edu.cn;

刘 刚，教授. E-mail: liugang@upc.edu.cn

作者简介: 李东泽，博士生. E-mail: B19060007@s.upc.edu.cn

本文的电子版全文由 Elsevier 出版社在 ScienceDirect 上出版（https://www.sciencedirect.com/journal/new-carbon-materials/）

Guide for Authors (1)

New Carbon Materials is a bimonthly journal published with the permission of the Ministry of Science and Technology and of the State News and Publication Agency. The journal is sponsored by the lnstitute of Coal Chemistry, Chinese Academy of Sciences, and is published by Science Press.

Aims and Scope

New Carbon Materials publishes research devoted to the physics, chemistry and technology of those organic substances that are precursors for producing aromatically or tetrahedrally bonded carbonaceous solids, and of the materials that may be produced from those organic precursors. These materials range from diamond and graphite through chars, semicokes, mesophase substances, carbons, carbon fiters, carbynes, fullerenes and carbon nanotubes, tec. Papers on the secondary production of new carbon and composites materials (for instance, carbon-carbon composites) from the above mentioned various carbons are also within the scope of the journal. Papers on organic substances will be considered if research has some relation to the resulting carbon materials.

Manuscript Requirements

1. *New Carbon Materials* accepts Research Paper, Short Communication and Review. The number of words in each Research Paper should be less than 8 000 words. Short Communication <4 500 words. There is no maxium of words for Review.

2. Manuscript including an abstract, graphical abstract, highlight, keywords, reference list, original figures and captions, tables. The figures can be edited by Origin. And the resolution of TEM, SEM, AFM, etc. images should be high.

3. Manuscript should be accompanied with key words placed after Abstract and a short resume of first author (name, academic degree, professional position) placed in the end of 1st page of text as foot-note. Corresponding author and his (her) E-mail address should also be mentioned.

4. All illustrations, photographs, figures and tables should be on separate sheets, figure captions should be typed separately, not included on the diagram. Authors are requested to submit original photographs, which should have good contrast and intensity.

5. References should be individually numbered in the order in which they are cited in the text, and listed in numerical sequence on separate sheets at the end of the paper, typed in double spacing. Remember that "unpublished works" are not references! In the reference list, periodicals [1], books [2], multi-author books with editors [3], proceedings [4], patents [5], and thesis [6] should be cited in accordance with the following examples:

[1] Kandalkar S G , Dhawale D S, Kim C K, et al. Chemical synthesis of cobalt oxide thin film electrode for supercapacitor application[J]. Synthetic Metals, 2010, 160(11): 1299-1302.

[2] lnagaki M, Kang F Y.Carbon Materials Science and Engineerng-From Fundamentals to Applications[M]. Beijing: Tsinghua University Press, 2011: 3-6.

[3] Toropov V V, Jones R, Willment T, et al. Weight and manufacturability optimization of composite aircraft components based on a genetic algorithm[P]. 6th World Congresses of Structural and Multidisciplinary Optimization, Rio de Janeiro, Brazil, 2005, 30.

[4] Yang H. Deposit, doping and photocatalytic activity of fibrous TiO2[D]. Dalian University of Technology, 2007.